Project Mountainwell
Interim Technical Report No. 9

PERFORMANCE AND OPTIMIZATION OF ARCAS AND OTHER SINGLE-STAGE ROCKETS WITH VACUUM-AIR BOOST

by

Sudhir Kumar
Stanley Chin-nan Shieh

August 1969

U. S. Army Research Office-Durham
Box CM, Duke Station
Durham, North Carolina

ABSTRACT

Studies on optimization of a single-stage rocket performance with and without the use of the Vacuum-Air Missile Boost (VAMB) system are presented here. Optimization is defined as maximizing the altitude to which a certain rocket of a given weight and propellant can send a fixed payload. Standard atmosphere has been used for the analysis. Performance estimation and optimization of a hypothetical 1,000 lb rocket with and without the VAMB system have been done under the simplifying assumptions of constant (neglecting the pressure thrust) for the powered flight and a constant drag coefficient for the whole flight. Similar studies have also been performed for eighteen real rockets without the VAMB system. It was found that the optimum thrust-to-weight ratio (T/W) for conventional rocket can be estimated roughly for preliminary design of rockets under these assumptions. The maximum altitude reached is, however, underestimated by this approach. For launch of rockets utilizing the VAMB system, determination of optimum T/W is also important. It becomes critical when the loading density of the rocket is low ($\leq$10), its fuel ratio approaches unity and the initial velocity imparted is high ($\geq$500 fps). Detailed performance and optimization studies have been presented

on the Arcas rocket. These are based on measured data of thrust and drag coefficient variations for a recent Arcas design, as obtained from the White Sands Missile Range. It was found that the optimum T/W for Arcas with and without VAMB system is approximately 2.4, which is almost half of the present design value (4.5). The gain in maximum altitude of the optimized Arcas launched with an initial velocity of 1,000 fps, over that of the present design Arcas without booster, was estimated to be nearly 93 per cent. It is concluded that the VAMB system is a very helpful adjunct to small rockets of optimized design.

CONTENTS

LIST OF FIGURES

List of Figures Cont'd.

LIST OF TABLES

NOTATIONS

Symbol	Description	Unit
T/W	Thrust-to-weight ratio	-
$(T/W)_{opt}$	Optimum thrust-to-weight ratio	-
Y_{max}	Maximum altitude	ft
Y_0	Initial altitude	ft
Y_b	Burnout altitude	ft
Y, y	Altitude	ft
V_{av}	Average velocity of rocket	fps
V	Velocity	fps
V_0	Initial velocity	fps
V_b	Burnout velocity	fps
V_g	Exhaust velocity of ejected gas	fps
T	Total thrust	lb
T_{sL}	Sea-level thrust	lb
$\bar{T}_{sL}$	Average sea-level thrust	lb
T_a	Atmospheric temperature	^oR
T_0	Stagnation temperature	^oR
$(T_0)_{max}$	Maximum stagnation temperature	^oR
p, p_a	Ambient atmospheric pressure	lb/ft^2

Notations cont'd.

Symbol	Description	Unit
P_{SL}	Atmospheric pressure at sea-level	lb/ft^2
W	Lift-off weight	lb
$\dot{w}$	Propellant flow rate	lb_m/sec
W_p	Weight of propellant	lb
m	Instantaneous mass of rocket	slug
A	Frontal area of rocket	ft^2
A_e	Effective area of nozzle exit	ft^2
D	Aerodynamic drag force	lb
d	Diameter of rocket	in
C_D	Drag coefficient	-
ρ	Atmospheric density	lb_m/ft^3
g	Gravitational acceleration	ft/sec^2
t	Time	sec
t_b	Burnout time	sec
ω	Angular velocity of earth rotation	rad/sec
ϕ	Latitude	degree
x, z	Distance deflected from local vertical	ft
P_s	Stagnation pressure	lb/ft^2
C_p	Specific heat at constant pressure	$Btu/lb-^oF$
Q	Integrated drag	lb-sec
I_{sp}	Specific impulse	sec
F_R	Fuel ratio	-
M	Mach number	-

Notations cont'd.

Symbol	Description	Unit
$(\ )_{V_0}$	With an initial velocity	-
$(\ )_{V_0 = 0}$	Without initial velocity	-
R	Earth's radius	ft
R_0	Gas constant for air	$lb\text{-}ft/lb_m\text{-}^oR$

ACKNOWLEDGMENT

The authors are thankful to Mr. William Reiter for having assisted in some earlier work of this report. They are also obliged to Dr. Louis Duncan, of U. S. Army White Sands Missile Range, for providing extensive data and characteristics of the Arcas rocket. Special thanks are also due to Mrs. Patricia Russell for her excellent typing.

PERFORMANCE AND OPTIMIZATION OF ARCAS AND OTHER SINGLE-STAGE ROCKETS WITH VACUUM-AIR BOOST

CHAPTER I

INTRODUCTION

The vacuum-air missile boost system was developed earlier[1,2,3,4,5,6,7] for the boosting of small to medium size solid propellant rockets, by imparting them an initial velocity at launch. Most of the previous work was concerned with the flow mechanics and dynamics of the missile inside the tube. Thus, reliable estimates of the velocities, which can be imparted to a certain rocket by this system, can be made. The problem of optimizing the rocket performance by utilizing this system, however, remains unsolved. This thesis essentially studies some of these aspects with special reference to a particular rocket, the Arcas (All Purpose Rocket for Collecting Atmospheric Soundings).

The vacuum-air missile boost system, later referred to as the VAMB system, consists of a partially evacuated vertical launching tube with a breakable seal at the top and with the lower end sealed by the missile on a held-down sabot. When the sabot is released, atmospheric pressure from air entering the base of the tube accelerates the missile. A muzzle chamber near the top of the tube reduces the velocity loss due to compression

of the residual air above it, and the tube length beyond the muzzle chamber serves as an atmospheric shock reducer. The velocity imparted by this system can be up to the sonic velocity. The VAMB system is considered suitable for upper-atmospheric sounding rockets. Some of the advantages of the system when compared to the usual surface-launching technique are a significant fuel saving or an increase in payload[8], less sensitivity to surface gusts, and a shelter prior to firing.

Much work has been done on the optimum performance of the usual surface-launching rockets[9,10,11,12]. For optimization of the performance of a rocket launched by the VAMB system, the present study was initiated to investigate the effects of the various rocket parameters. Variations of parameters, such as initial thrust-to-weight ratio and fuel ratio, on the performance of sounding rockets have been studied. Essentially, the main problem considered herein is that of determining rocket burning programs that use a given amount of fuel to propel a given mass to a maximum altitude. Or putting it differently, the criterion of optimization, for this investigation, is to maximize the altitude to which a given payload can be sent by a rocket of a specified weight.

Preliminary study was conducted with a hypothetical rocket of 1,000 lb. with characteristics similar to comparable weight rockets. A wide variety of real rockets were then investigated. Further refined study was made specially for the single-stage Arcas rocket currently in use. Finally, forward stagnation temperatures and pressures of the Arcas rocket during optimum performance were evaluated.

Results of this investigation indicate that a significant gain in maximum altitude can be attained by simultaneous optimization of the thrust-to-weight ratio and application of the VAMB system.

CHAPTER II

FORMULATION OF THE EQUATIONS OF MOTION

2.1 Simplified Equations of Motion for Vertical Trajectory

In developing the equations of motion for the vertical flight of a single-stage rocket in an atmosphere near the earth's surface, the following assumptions are made:

i) The earth's gravitational field is constant and the gravitational acceleration is taken to be 32.2 ft/sec^2, the value at the sea-level. Although it decreases with increasing altitude, the error induced is about 10 per cent at the altitude of 200 miles which is the extreme altitude within our scope of study.

ii) The density and pressure of the atmosphere vary parabolically with the altitude up to 55,000 ft. and exponentially above this altitude. The expressions for the variations fit the experimental data fairly closely as described in Sec. 3.2.

iii) The rocket propellant is consumed at a constant rate. This is generally accepted by rocket designers.

iv) The exhaust velocity of the burned gases relative to the rocket is constant. This is quite reasonable for most rockets.

v) The thrust direction is aligned with the rocket longitudinal axis which always remains vertical. For vertical flight, this assumption is quite acceptable.

vi) Effects of the earth's rotation are neglected. This is to be justified in the following section.

vii) Effects of the atmospheric winds are neglected. The wind speed is difficult to estimate and its magnitude is much smaller than the velocity of the rocket thus having little effect on the trajectory.

viii) Only thrust, aerodynamic drag force, and gravity affect the motion since other forces are small compared to these.

ix) The aerodynamic drag force is given by

$$D = \frac{1}{2} C_D \rho A V^2$$

where A, V are the frontal area and the velocity of the rocket; C_D is the drag coefficient which may be a constant or a variable (a function of Mach number); and ρ, the ambient air density in slug/ft^3, is a function of altitude.

Under these assumptions the equation of motion for a vertical trajectory during burning (sustain phase) is written as

$$\frac{dV}{dt} = \frac{T - D}{(W - wt)/g} - g$$

or

$$\frac{dV}{dt} = \frac{(T/W)\, g}{1 - \frac{wt}{W}} - \frac{Dg}{W - wt} - g \qquad (2\text{-}1)$$

where

T = thrust = $\dot{w} V_g/g + A_e (P_{sL} - P_a)$ (2-2)

D = aerodynamic drag = $\frac{1}{2} C_D \rho A V^2$ (2-3)

W = lift-off weight

$\dot{w}$ = propellant flow rate in lb_m/sec

t = time

g = gravitational acceleration

V_g = exhaust velocity of ejected gas

A_e = effective area of nozzle exit

P_{sL} = atmospheric pressure at sea-level

P_a = ambient pressure of atmosphere

Also by definition

$$\frac{dY}{dt} = V \qquad (2-4)$$

where

Y = altitude in feet.

In Eq. (2-2), the thrust includes pressure thrust, $A_e (P_{sL} - P_a)$, in addition to momentum thrust, $\dot{w}V_g/g$. The pressure thrust, usually not so important. is only a few per cent of the momentum thrust and hence, is neglected in the preliminary study.

Once burning is terminated, only aerodynamic drag and gravity affect the free flight (coasting phase) of the rocket and the equation of motion reduces to

$$\frac{dV}{dt} = - \frac{Dg}{W - W_p} - g \qquad (2-5)$$

where W_p is the weight of the propellant.

Equations (2-1) and (2-4) are to be solved for the altitude Y during burning. Once the free flight begins, Eqs. (2-4) and (2-5) are used to solve for Y during the vertical ascent. These equations apply only to the ascending rocket and are not valid for its free fall to the earth's surface.

The initial conditions required to solve for Y during the powered and the free flight phases are:

$$0 \leq t \leq t_b$$
$$V(0) = V_0 \qquad (2\text{-}6)$$
$$Y(0) = Y_0$$

for powered flight, and

$$t_b < t \leq t_f$$
$$V(t_b) = V_b \qquad (2\text{-}7)$$
$$Y(t_b) = Y_b$$

for free flight.

In Eqs. (2-6) and (2-7), the subscripts 0, b, and f refer to the conditions at launch, at burnout and at maximum altitude respectively.

2.2 Rotational Effects of the Earth

The equations of motion previously derived are based on

the assumption of earth-fixed coordinate system. A simplified analysis of the earth's rotational effects on the maximum altitude of the missile is presented in this section.

It is assumed that a coordinate system XYZ, the origin of which is fixed at the earth's center and the axes of which are fixed with respect to the fixed stars with Z-axis along the earth's axis of rotation, represents an inertial system. A coordinate system xyz with the origin at the launch point and axes along ϕ, R, θ directions is attached to the earth's surface. The unit vectors $\bar{i}$, $\bar{j}$, $\bar{k}$ are associated with x, y, z axes respectively. These coordinate systems are shown in Fig. 2-1. Then, the position vector of the missile relative to 0 is

$$\bar{r} = \bar{R} + \bar{S} \tag{2-8}$$

Since 0 is a fixed point in an inertial frame, the absolute acceleration of the missile is

$$\ddot{\bar{r}} = \ddot{\bar{R}}\Big|_{xyz} + \ddot{\bar{S}}\Big|_{xyz}$$

or

$$\ddot{\bar{r}} = \dot{\bar{\omega}} \times \bar{R} + \bar{\omega} \times \bar{\omega} \times \bar{R} + \dot{\bar{\omega}} \times \bar{S} + 2\bar{\omega} \times \dot{\bar{S}}\Big|_{xyz} + \ddot{\bar{S}}\Big|_{xyz} \tag{2-9}$$

since $\dot{\bar{R}} = \dot{\bar{\omega}} = 0$.

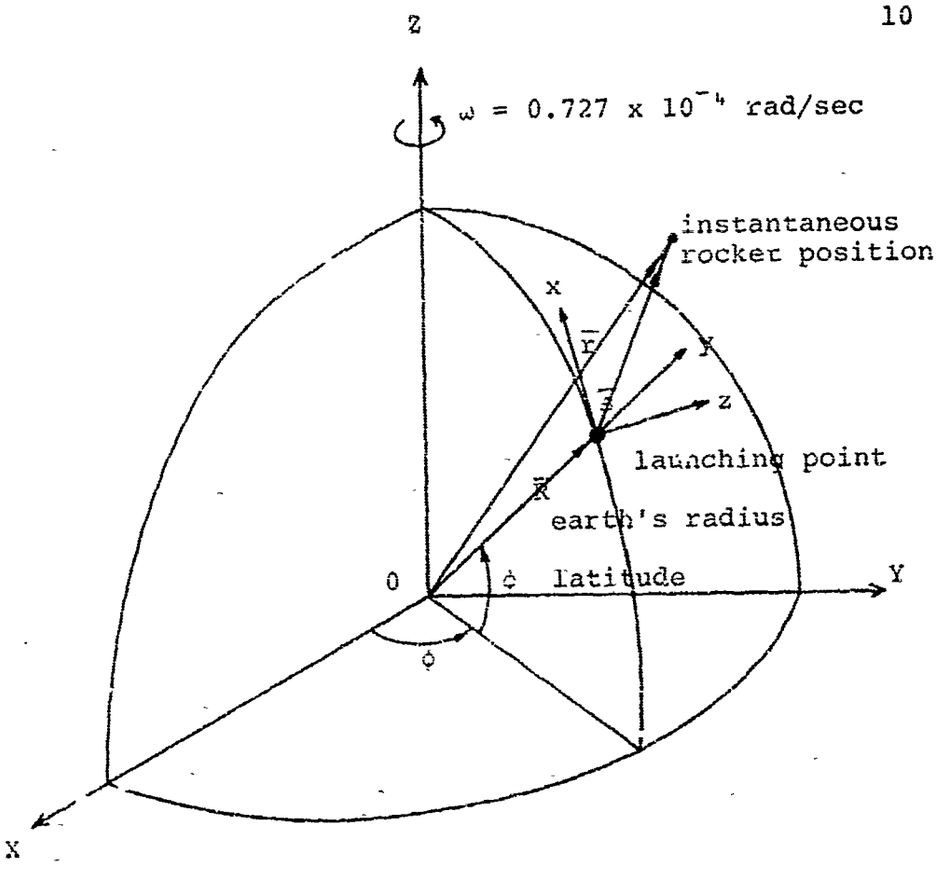

Fig. 2-1.a. Inertial coordinate system XYZ fixed in space.

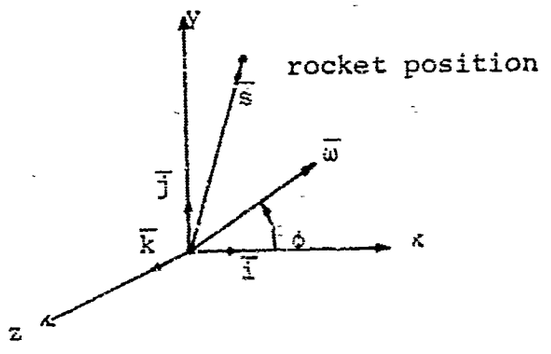

Fig. 2-1.b. Coordinate system attached to the rotating earth, x and z tangential to the earth surface.

In general, $\bar{\omega} \times \bar{\omega} \times \bar{S}$ is small compared to $\bar{\omega} \times \bar{\omega} \times \bar{R}$, and thus may be neglected. This is based on the argument that S is of the order of 200 miles or less while R is of the order of 4,000 miles. Furthermore, one may, with little loss of accuracy, assume that the external forces - thrust, drag and gravity - are acting in the direction of local vertical, i.e., along the y-axis. The equation of motion in the inertial coordinate system is then written as

$$(T - D - mg)\bar{j} = m\left[\bar{\omega} \times \bar{\omega} \times \bar{R} + 2\bar{\omega} \times \dot{\bar{S}}\Big|_{xyz} + \ddot{\bar{S}}\Big|_{xyz}\right] \qquad (2\text{-}10)$$

Introducing $\bar{\omega} = \omega\cos\phi\ \bar{i} + \omega \sin\phi\ \bar{j}$,
one obtains the scalar form of the equations of motion in the coordinate system xyz as follows:

$$x: \quad 0 = m\left[\omega^2 R \sin\phi \cos\phi + 2\omega\dot{z}\sin\phi + \ddot{x}\right] \qquad (2\text{-}11)$$

$$y: \quad T - D - mg = m\left[-\omega^2 R \cos^2\phi - 2\omega\dot{z}\cos\phi + \ddot{y}\right] \qquad (2\text{-}12)$$

$$z: \quad 0 = m\left[2\omega(\dot{y}\cos\phi - \dot{x}\sin\phi) + \ddot{z}\right] \qquad (2\text{-}13)$$

The rocket is travelling nearly vertically upwards, so $\dot{x} << \dot{y}$ and $\dot{z} << \dot{y}$, and the products $\omega\dot{x}$ and $\omega\dot{z}$ are vanishingly small because of the smallness of $\omega(0.727 \times 10^{-4}$ rad/sec). Thus, the Eqs. (2-11) through (2-13) reduce to

$$0 = \omega^2 R \sin\phi \cos\phi + \ddot{x} \qquad (2\text{-}14)$$

$$T - D - mg = m\left[-\omega^2 R \cos^2\phi + \ddot{y}\right] \qquad (2\text{-}15)$$

$$0 = -2\omega\dot{y}\cos\phi + \ddot{z} \qquad (2\text{-}16)$$

In examining Eq. (2-15), the centrifugal acceleration, $\omega^2 R = 0.11$ ft/sec^2, is only 0.003g and thus may well be neglected. Since, even for a long time of flight, say 200 seconds, its contribution to the altitude only reaches 2,200 feet which is no more than one per cent of the maximum altitude. Therefore, Eq. (2-15) reduces to the same form as derived by assuming non-rotating earth. This justifies the assumption that the earth's rotation has little effect on the maximum altitude of the missile within our scope of study.

It can be seen from Eqs. (2-14) and (2-16) that the deflections in the x and z directions depend on the latitude of the launch spot, ϕ.

In the x-direction, there would be no deflection if launching is done at the equator or at the poles. If $\phi = 45^{\circ}$, however, it reaches the maximum and Eq. (2-14) becomes

$$\ddot{x} = -0.5\,\omega^2 R$$

Upon integration one obtains

$$x = -0.25\,\omega^2 R t^2$$

or

$$x = -0.0276t^2 \qquad (2\text{-}17)$$

For various times of flight, the deflections in the x-direction for $\phi = 45^\circ$ are indicated below (Table 2-1).

The deflection in the z-direction vanishes as $\phi = 90^\circ$, while it reaches its maximum as $\phi = 0^\circ$ (at the equator). It can be estimated by taking an average velocity, $\dot{y}_{av}$, during the flight so that Eq. (2-16) may readily be integrated. By doing so, one obtains

$$z = -\omega \dot{y}_{av} \cos\phi \, t^2 \qquad (2\text{-}18)$$

The deflections in the z-direction for various times of flight and average velocities are presented in Table 2-2.

The simplified analysis of the earth's rotational effects, which has so far been conducted, indicates that the earth's rotation has little effect on the maximum altitude of the missile at least within our scope of study, and hence has no significant contribution to Y_{max}. The deflections of the missile in the x and z directions, however, can be of considerable significance for long time of flight in certain launching areas as indicated in Tables 2-1 and 2-2.

Table 2-1. Deflections in the x-direction for various times of flight, $\theta = 45^{\circ}$.

time of flight t sec.	x-deflection -x ft.
30	25
60	100
90	224
120	398
150	622
180	895

Table 2-2. Deflections in the z-direction for various times of flight and average velocities, $\phi = 0^{o}$ and $\phi = 45^{o}$.

average velocity $\dot{y}_{av}$ fps	time of flight t sec	z-deflection - z ft $\phi = 0^{o}$	z-deflection - z ft $\phi = 45^{o}$
1,000	30	65	46
	60	262	185
	90	589	416
	120	1,050	743
	150	1,640	1,160
	180	2,350	1,660
2,000	30	130	92
	60	524	370
	90	1,178	832
	120	2,100	1,486
	150	3,280	2,320
	180	4,700	3,320
3,000	30	195	138
	60	786	555
	90	1,767	1,248
	120	3,150	2,230
	150	4,920	3,480
	180	7,050	4,980

CHAPTER III

NUMERICAL PROCEDURE AND DESCRIPTION OF THE ATMOSPHERE

3.1 Numerical Procedure

By varying the thrust-to-weight ratio of a single-stage rocket of a given size, it is intended in this study to deliver a certain payload to the maximum altitude. This is used as the criterion of optimization of small single-stage rockets for this study.

It is obvious that gravity loss and drag loss significantly influence the maximum altitude. The drag loss increases with increasing thrust-to-weight ratio while the gravity loss decreases with increasing thrust-to-weight ratio. Theoretically, minimizing the losses due to gravity and drag will maximize the altitude. The complexity of the non-linear differential equations of motion, however, makes it impossible to obtain an analytical mathematical expression for this. Therefore, numerical integration methods become necessary to solve the equations. Runge-Kutta method of the fourth order[13] is selected, and the calculations are conducted with the aid of a digital computer.

In determining the optimum thrust-to-weight ratio for a specified rocket with an initial velocity imparted by the VAMB system, rocket parameters such as lift-off weight, specific impulse, fuel ratio (ratio of weight of propellant to lift-off weight), and frontal area are fixed while the thrust-to-weight ratio is varied. Change of thrust-to-weight ratio is related to a definite change in burning time or flow rate, area of nozzle exit, and curve for variations of drag coefficient with Mach number during burn phase.

With some specified thrust-to-weight ratio and rocket characteristics, one can readily compute the weight of propellant, propellant flow rate, and burning time. Having this information, the equations of motion can be integrated numerically to obtain a value for maximum altitude.

One then changes the thrust-to-weight ratio, and computes the new values of flow rate, burning time, area of nozzle exit, and C_D curve during burn phase. The equations of motion are integrated again to produce a new value of maximum altitude. This procedure is repeated for a selected range of thrust-to-weight ratios. A curve is thus plotted for maximum altitude versus thrust-to-weight ratio and the peak on the curve locates the optimum thrust-to-weight ratio for the specific rocket under the specified launching conditions.

Before numerical analyses proceed, the definition of thrust-to-weight ratio should be identified. It is defined as the ratio of average sea-level thrust (assuming optimum nozzle for sea-level operation) to lift-off weight. Under this definition, the thrust only includes the momentum thrust. Thus,

the definition actually means the initial thrust-to-weight ratio.

The specific impulse is defined as the averag sea-level thrust per unit flow rate. Therefore

$$I_{sp} = \bar{T}_{SL}/\dot{W} = V_g/g$$

And so, I_{sp} is constant for a given rocket.

3.2 Properties of the Atmosphere

One of the important forces affecting the motion of the rocket is aerodynamic drag which depends on velocity, frontal area, drag coefficient and air density. The drag coefficient is a function of Mach number, which is, in turn, connected with the temperature of air. Therefore, variations of atmospheric properties with altitude must be taken into consideration.

1) Descriptions of density and pressure

A least squares curve fit was used to develop expressions for air density as a function of altitude from a sequence of experimental data[1] (altitudes from sea-level to 100,000 ft). The best fit was obtained by using a polynomial of the form

$$\rho = C_3 - C_1 Y + C_2 Y^2 \qquad (3\text{-}1)$$

for altitudes of 55,000 ft. or less, and an exponential form

$$\rho = \rho_1 \, e^{\alpha Y} \qquad (3\text{-}2)$$

for altitudes above 55,000 ft.

The constants obtained from a least squares curve fit program are

$C_0 = 0.757878 \times 10^{-1}$

$C_1 = -0.203365 \times 10^{-5}$

$C_2 = 0.150855 \times 10^{-10}$

$\rho_1 = 0.129184$

$\alpha = -0.480263 \times 10^{-4}$

These constants will give the atmospheric density as a function of altitude in lb_m/ft^3.

Similar approach was applied to variations of the atmospheric pressure in lb/ft^2 and the resulting expressions are

$$P = a_0 + a_1 Y + a_2 Y^2 \qquad (3\text{-}3)$$

for $Y \leq 55{,}000$ ft, and

$$P = P_1 \, e^{\gamma Y} \qquad (3\text{-}4)$$

for $Y > 55{,}000$ ft.

The constants were found as follows:

$a_6 = 0.208393 \times 10^{-}$

$a_1 = -0.[illegible]6794 \times 10^{-3}$

$a_2 = 0.5961o8 \times 10^{-6}$

$a_3 = 0.265263 \times 10^{-}$

$a_4 = -0.478109 \times 10^{-}$.

The approximate curves for variations of atmospheric density and pressure, as shown in Figs. 3-1 and 3-2 respectively, fit the experimental data fairly closely.

ii) Description of temperature

With density and pressure calculated from the above expressions, the temperature (in ^{o}R) of atmosphere is given by the perfect gas law

$$P = \rho R_o T_a$$

or

$$T_a = P/\rho R_o \qquad (3-5)$$

in which, R_o is the gas constant.

Since both density and pressure decrease with increasing altitude, they become very small when altitude is 120,000 ft. or more. Thus, the temperatures computed fror the perfect gas law may deviate from the experimental data significantly. In order to obtain more accurate values, the following expressions, approximated from experimental data[11], are adopted.

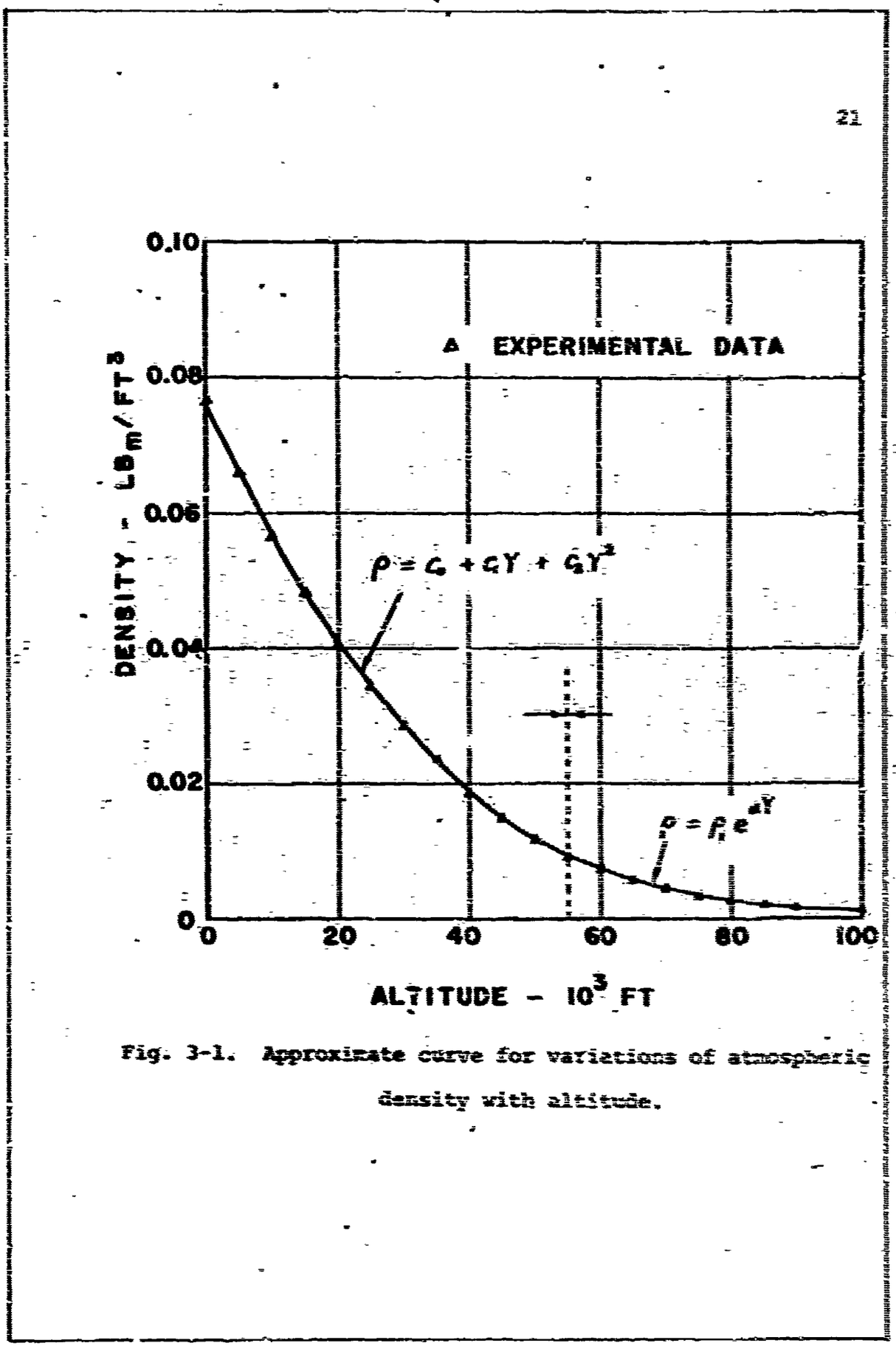

Fig. 3-1. Approximate curve for variations of atmospheric density with altitude.

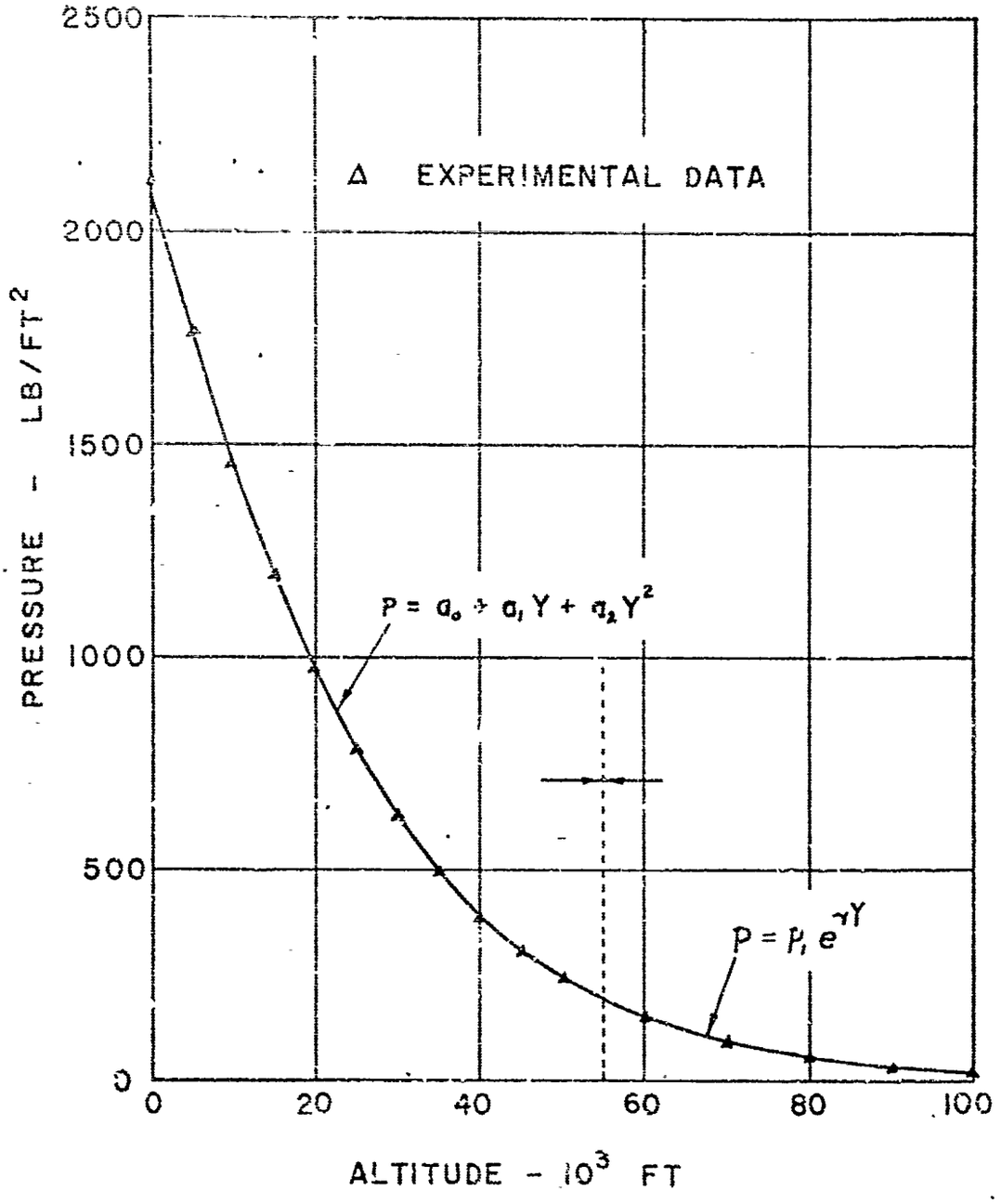

Fig. 3-2. Approximate curve for variations of atmospheric pressure with altitude.

For 120,000 ft $\leq$ Y $\leq$ 164,000 ft,

$$T_a = 450 + \frac{180}{44,000} \quad (Y - 120,000) \tag{3-6}$$

For 164,000 ft < Y $\leq$ 200,000 ft,

$$T_a = 630 \ ^{o}R \tag{3-7}$$

And, for 200,000 ft < Y $\leq$ 250,000 ft,

$$T_a = 450 + \frac{180}{50,000} \ (250,000 - Y) \tag{3-8}$$

Since experimental data for temperature are not available for altitudes higher than 250,000 ft, it was considered necessary to resort to the perfect gas law to estimate the temperature above this altitude.

CHAPTER IV

INFLUENCE OF VARIOUS PARAMETERS ON THE PERFORMANCE OF A HYPOTHETICAL ROCKET AND SOME REAL ROCKETS UNDER SIMPLIFYING ASSUMPTIONS

4.1 Introductory Comments

As mentioned before, the complexity of the equations of motion makes it impossible to obtain an analytical mathematical expression for the maximum altitude. Accurate solutions are obtained only by using a digital computer, but each of these applies to a certain rocket under some specified launching conditions. However, by examining performances of many rockets, the tentative influence of rocket parameters still can be revealed. It is the purpose of this chapter to investigate a variety of real rockets to acquire some general ideas concerning the performance of the rocket.

For simplifying the analysis, two assumptions are made in this preliminary study:

i) Only the momentum thrust is considered and it is assumed to be constant throughout the burn phase. The pressure thrust due to the variation of altitude is neglected since it is only a few per cent of the momentum thrust.

ii) An estimated constant drag coefficient is assumed throughout the vertical ascent of the rocket.

Although these assumptions are not valid for the actual performance of the rocket, results are yet considered helpful in parametric studies.

Numerical integration with time step of 0.5 seconds has been conducted with the aid of a digital computer. First of all, a hypothetical rocket of 1,000 lb is investigated, and then a number of real rockets are studied.

4.2 Hypothetical rocket of 1,000 lb

The Aerobee rocket was the first rocket of its type developed specifically to investigate the upper atmosphere and was for a long time practically the only readily available upper-atmospheric sounding rocket in the United States. For this reason, an imaginary rocket with characteristics comparatively similar to the Aerobee is adopted to look into the performance of the sounding rocket. Some characteristics involved in the analysis of this hypothetical rocket are listed below:

Lift-off weight, W = 1,000 lb

Diameter, d = 13.55 in.

Fuel ratio (ratio of weight of propellant to lift-off weight), F_R = 0.7

Specific impulse, I_{sp} = 200 sec

Drag coefficient, C_D = 0.4.

With a specified thrust-to-weight ratio and an initial velocity, one can integrate numerically the equations of motion to determine the maximum altitude reached by the rocket. Thrust-to-weight ratios in the range of 1 through 12 and initial velocities of 0, 500, and 1,000 fps were selected in the computations. Computational results are plotted with thrust-to-weight ratios as abscissas and maximum altitudes as ordinates, as shown in Fig. 4-1. The time integral of the aerodynamic drag, defined as

$$Q = \int_0^{t_f} (\text{Drag})\, dt, \qquad (4\text{-}1)$$

and its relationship with the rocket performance, was also studied.

Figure 4-1 shows that the optimum thrust-to-weight ratio, $(T/W)_{opt}$, is located around 2.7 irrespective of initial velocities, and the altitude increases 56 per cent due to an imparted initial velocity of 1,000 fps at this thrust-to-weight ratio. The slopes of the Y_{max} versus T/W curves are much steeper for values of $T/W < (T/W)_{opt}$ in comparison with the case when $T/W > (T/W)_{opt}$. The plots of Q, the integrated drag, indicate that Q increases with T/W as expected. However, it is interesting to note that the Q plots for $V_0 = 0$ and $V_0 = 500$ fps are practically identical for $T/W < 5$. This implies that the total energy loss due to aerodynamic drag is not increased by imparting initial velocities up to 500 fps or more.

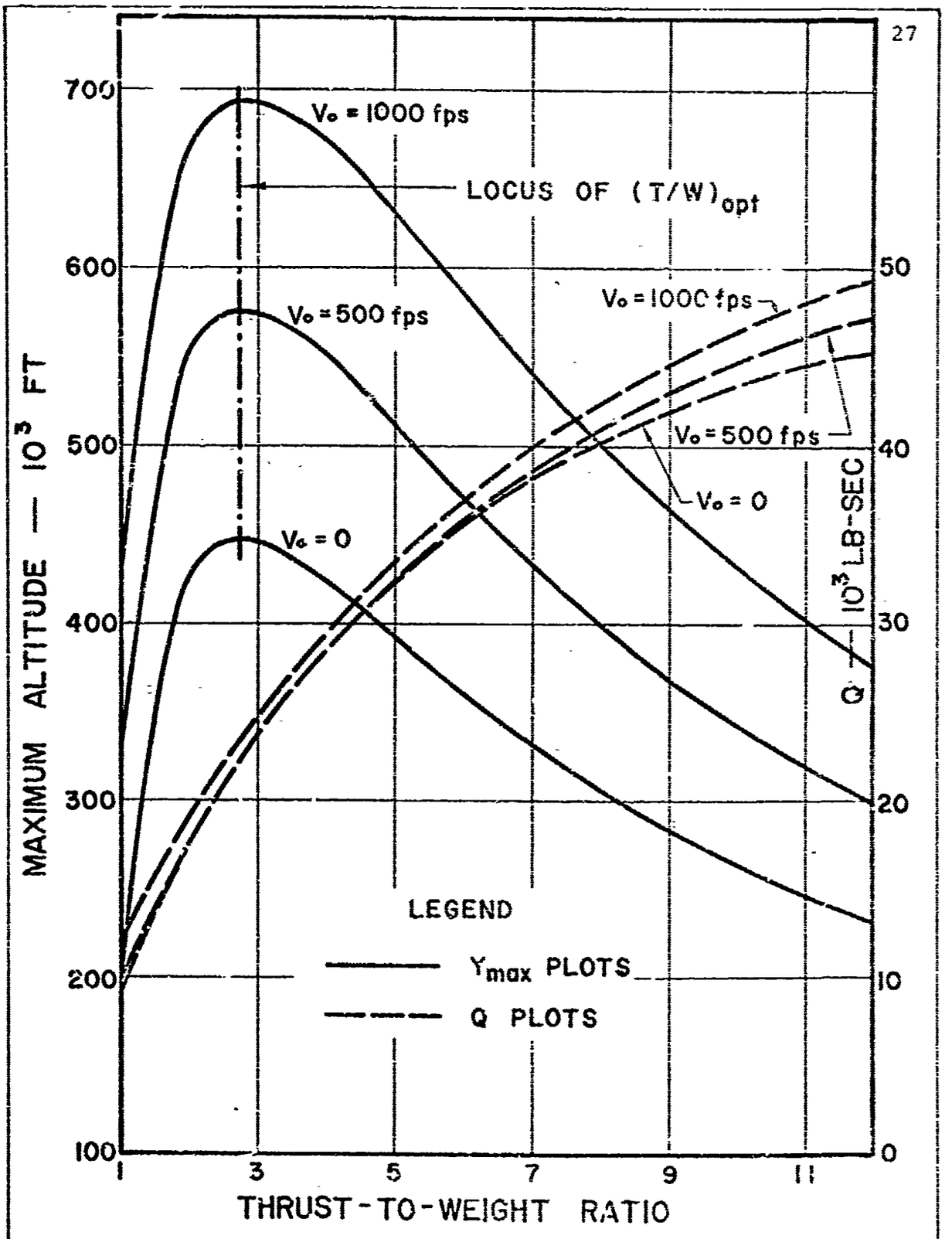

Fig. 4-1. Variations of maximum altitude and integrated drag with thrust-to-weight ratio for the hypothetical rocket, under simplifying assumptions (pressure thrust neglected and $C_D = 0.4$).

It is also interesting to examine the percentage increase in maximum altitude due to an initial velocity. It is defined as

$$\% \text{ increase in } Y_{max} = \frac{(Y_{max})_{V_0} - (Y_{max})_{V_0 = 0}}{(Y_{max})_{V_0 = 0}} \times 100 \qquad (4\text{-}2)$$

Computations have been made for different thrust-to-weight ratios. Figure 4-2 shows that the percentage increase in maximum altitude increases nearly linearly with the initial velocity. It should be indicated that the percentage increase in Y_{max} is minimum at the $(T/W)_{opt}$. This is no surprise because the Y_{max} at the $(T/W)_{opt}$ is much higher than that at the other T/W.

It is also interesting to observe the percentage increase in payload with the initial velocity. It is determined in two steps:

i) A maximum altitude is computed for a rocket launched with zero initial velocity.

ii) An initial velocity is specified. The fuel ratio is adjusted by trial and error until the maximum altitude computed for this rocket equals that computed in step i).

The net effect is an increase in the payload delivered to a specific altitude. In these computations, it is assumed that the weight of the rocket structure is 10 per cent of the weight of the propellant, W_p. It is defined that

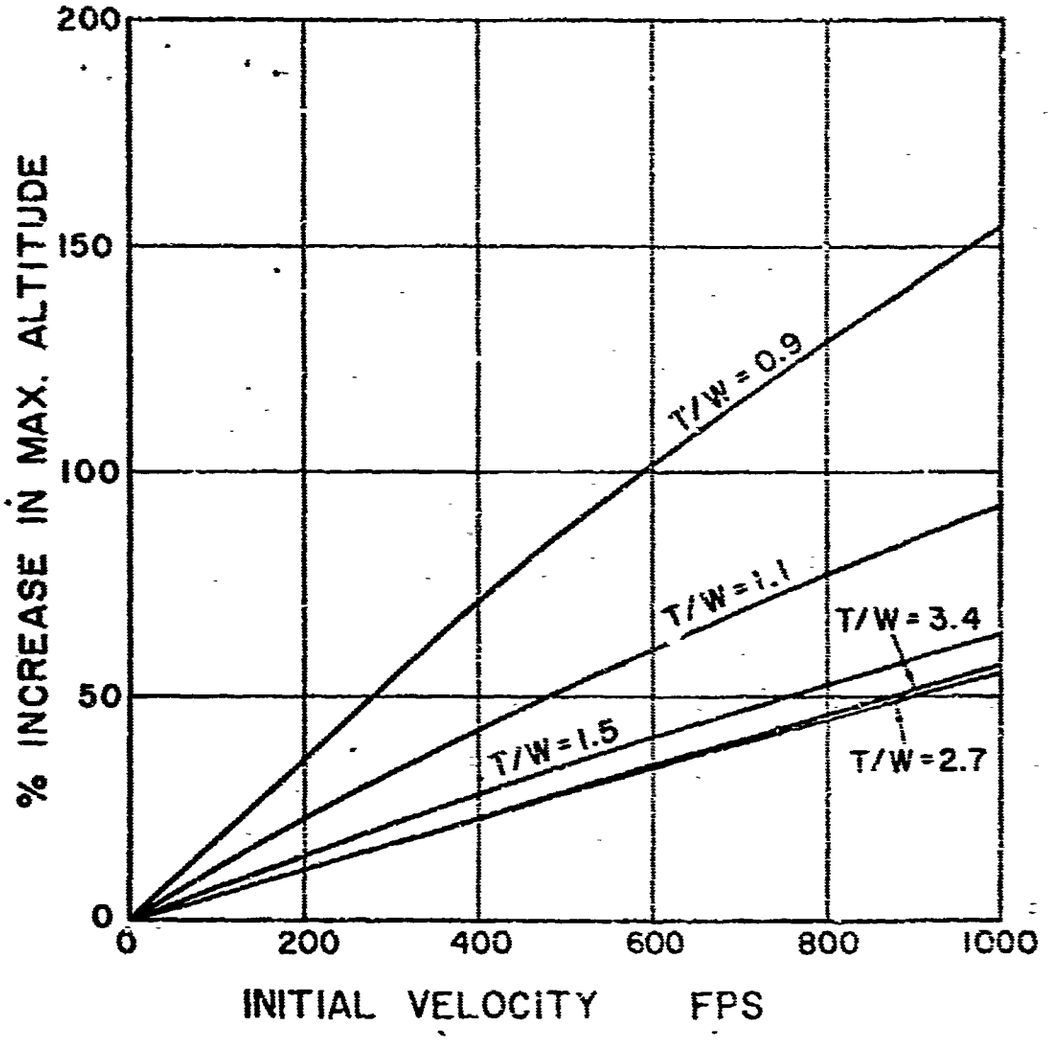

Fig. 4-2. Percentage increase in maximum altitude due to an initial velocity for the hypothetical rocket, under simplifying assumptions (pressure thrust neglected and $C_D = 0.4$).

$$\% \text{ increase in payload} = \frac{(\text{Payload})_{V_a} - (\text{Payload})_{V_a = 0}}{(\text{Payload})_{V_a = 0}} \times 100 \qquad (4\text{-}3)$$

This evaluation of the increase in payload is quite different from that made by Foa[3], who has assumed fixed burnout velocity instead of fixed Y_{max} and neglected the aerodynamic drag.

It is observed from Fig. 4-3 that the percentage increase in payload also increases nearly linearly with the inital velocity, and it is minimum when the thrust-to-weight ratio is at its optimum value.

Furthermore, in order to study the effect of the fuel ratio on the rocket performance, fuel ratios in the range of 0.4 to 0.8 were assumed for the hypothetical rocket. Plots of Y_{max} versus T/W for different fuel ratios are presented in Fig. 4-4. It can be seen from Fig. 4-4 that the $(T/W)_{opt}$ changes only slightly with the fuel ratio. However, the shapes of the curves are indeed modified. With the fuel ratio as low as 0.4, the curve for $T/W > (T/W)_{opt}$ is nearly flat. As the fuel ratio increases, the corresponding curve becomes steeper and steeper. This is due to the fact that the drag loss has much more significant effect than the gravity loss on the vertical ascent of the rocket having high fuel ratio. Thus, in this case, the performance of the rocket varies significantly with T/W and great care must be taken in determining the appropriate T/W for such a rocket.

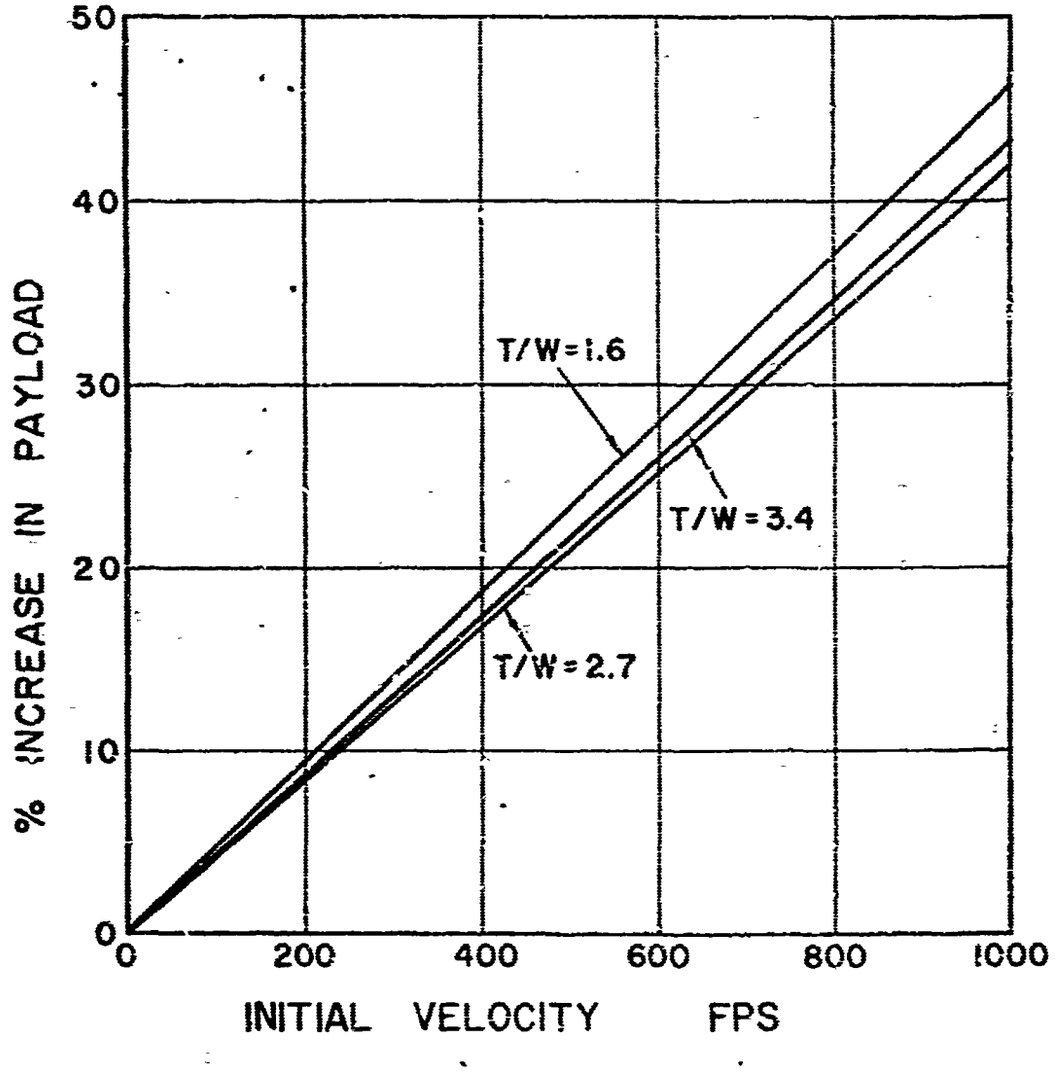

Fig. 4-3. Percentage increase in payload due to an initial velocity for the hypothetical rocket, under simplifying assumptions (pressure thrust neglected, $C_D = 0.4$, and weight of rocket structure = $0.1\ W_p$).

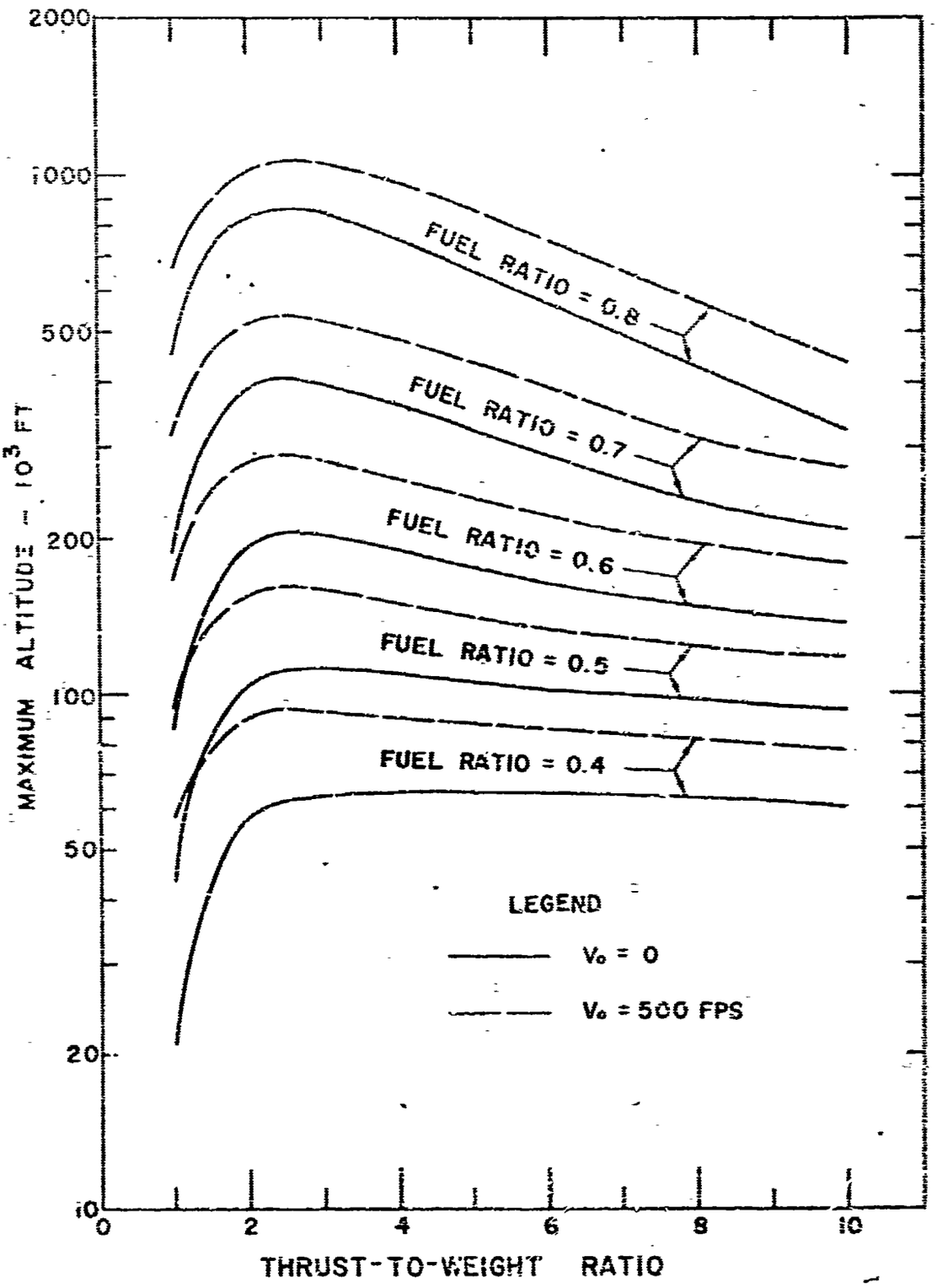

Fig. 4-4. Effect of fuel ratio on maximum altitude for the hypothetical rocket, under simplifying assumptions (pressure thrust neglected and C_D = 0.4).

The hypothetical rocket has so far been investigated under the assumptions of constant thrust (neglecting pressure thrust) for the burn phase and a constant drag coefficient throughout the vertical ascent. In fact, the rocket thrust increases with increasing altitude and the drag coefficient depends on Mach number. The maximum altitudes are, therefore, underestimated due to the neglect of pressure thrust and inaccurate estimate of constant drag coefficient. However, the $(T/W)_{opt}$ determined under these simplifying assumptions deviates only slightly from that determined by considering actual performance, as will be seen in Chapter V (Section 5.3 and Fig. 5-6).

On the basis of this investigation, the following observations may also be made:

i) The $(T/W)_{opt}$ seems not to vary significantly with the imparted initial velocity. In the present case, $(T/W)_{opt}$ = 2.7 for V_i = 0 to V_i = 1,000 fps.

ii) The Y_{max} decreases more drastically for $T/W < (T/W)_{opt}$ than for $T/W > (T/W)_{opt}$.

iii) The total energy loss due to aerodynamic drag increases with increasing T/W, but it does not increase significantly (= 13% for V_i = 1,000 fps) due to the imparted initial velocity. For the hypothetical rocket, Q, the total drag integral, is nearly the same for $0 < V_i < 500$ fps and $T/W < 5$.

iv) The percentage increase in Y_{max} increases nearly linearly with the initial velocity. It is minimum when $T/W = (T/W)_{opt}$. A 36 per cent increase is obtained by imparting an initial velocity of 1,000 fps at $(T/W)_{opt}$.

v) The percentage increase in payload also increases nearly linearly with the initial velocity. It is minimum when T/W = $(T/W)_{opt}$. A 42 per cent increase is attained by imparting an initial velocity of 1,000 fps at $(T/W)_{opt}$.

vi) The $(T/W)_{opt}$ alters only slightly with the fuel ratio. However, as the T/W increases beyond $(T/W)_{opt}$, the corresponding Y_{max} varies more with T/W for higher fuel ratio than for lower fuel ratio rockets. The closer the fuel ratio approaches unity, the steeper is the slope.

It is, therefore, considered feasible to estimate optimum T/W of real rockets under these simplifying assumptions, for preliminary design considerations. Final design parameters will still have to be based on more detailed analyses and computations utilizing actual wind tunnel test data. This is attempted as a second stage design analysis in the next chapter for one particular rocket, the Arcas.

4.3 Real Rockets

A wide variety of real rockets[15] listed in Table 4-1 were also investigated. The analyses were based on the simplifying assumptions of constant thrust (neglecting pressure thrust) and a constant drag coefficient. The drag coefficient was assumed to be 0.4, which is considered reasonable, for all rockets since detailed experimental data on these were not available. Computations were made with zero initial velocity and thrust-to-weight ratios in the range of 1 to 8. Curves of Y_{max} versus T/W for

Table 4-1. Characteristics of Real Rockets.

Rocket	W lb.	d in.	T/W	I_{sp} sec	F_R	W/d^2 lb/in.^{2}
Aerobee	1,070	15	2.43	185	0.59*	4.76
Aerobee Hi	1,300	15	3.08	200	0.77*	5.78
Aerobee 100	1,455	15	1.8	200	0.36*	6.42
Aerobee 150	2,093	15	1.96	198	0.5 *	9.3
Arcas**	70	4.45	4.5	315	0.43	3.5
Arcas (old)**	76.4	4.45	4.1	211	0.56	3.86
Aspan	1,500	16.5	3.9	210*	0.4 *	5.52
Exos	5,821	22.88	6.47	200*	0.4 *	11.1
Iris	1,128	12.13	4.0	230*	0.8 *	7.66
Meteo	1,500	17.3	2.01	173*	0.7 *	5.02
Nike-Cajun	1,550	16.5	6.2	200*	0.4 *	5.7
Pol 2	26,000	25	3.46	200*	0.7*	41.6
Skylark	2,560	17.6	4.5	192*	0.7*	8.27
Veronique AG-1	3,040	21.7	2.9	215	0.72*	6.46
Viking No. 1	9,650	32	2.12	165*	0.71	9.37
Viking No. 11	15,005	45	1.43	184*	0.8	7.41
V-2	27,376	65	2.05	205	0.69	6.47
Wac Corporal	665	12	2.25	195	0.52	4.62

* Estimated by the author, since data not available.
** Data from White Sands Missile Range, New Mexico.

these rockets are presented in Fig. 4-5.

The following observations can be made from the plots of Fig. 4-5:

i) For T/W < 2, the performance of most rockets, in terms of the Y_{max} attained, are degraded drastically.

ii) The curves become flat or inclined downwards as the thrust-to-weight ratios increase beyond the $(T/W)_{opt}$.

iii) The slope of the curve for $T/W > (T/W)_{opt}$ depends on the loading density term (W/d^2) and the fuel ratio. For the rockets having the same fuel ratio; the higher the W/d^2, the flatter the curve. For instance, the Pol 2 with $W/d^2 = 41.6$, the curve becomes nearly flat as T/W increases; on the other hand, the Meteo with $W/d^2 = 5.02$, the curve becomes inclined downwards. This results from the fact that the drag loss is much more significant than the gravity loss for those rockets having low values of W/d^2. Therefore, much care must be taken in determining the appropriate T/W for low W/d^2 value rockets since their performance is altered significantly by this parameter.

iv) Although some of these rockets have low values of W/d^2, their curves still look somewhat flatter than those for some other rockets with the same W/d^2. This is because their fuel ratios, F_R, are as low as 0.5 or less, which cause an opposite effect on the curves. However, the coupling of the effects of W/d^2 and F_R is difficult to establish, analytically or in a parametric form, because of the complexity of the rocket performance.

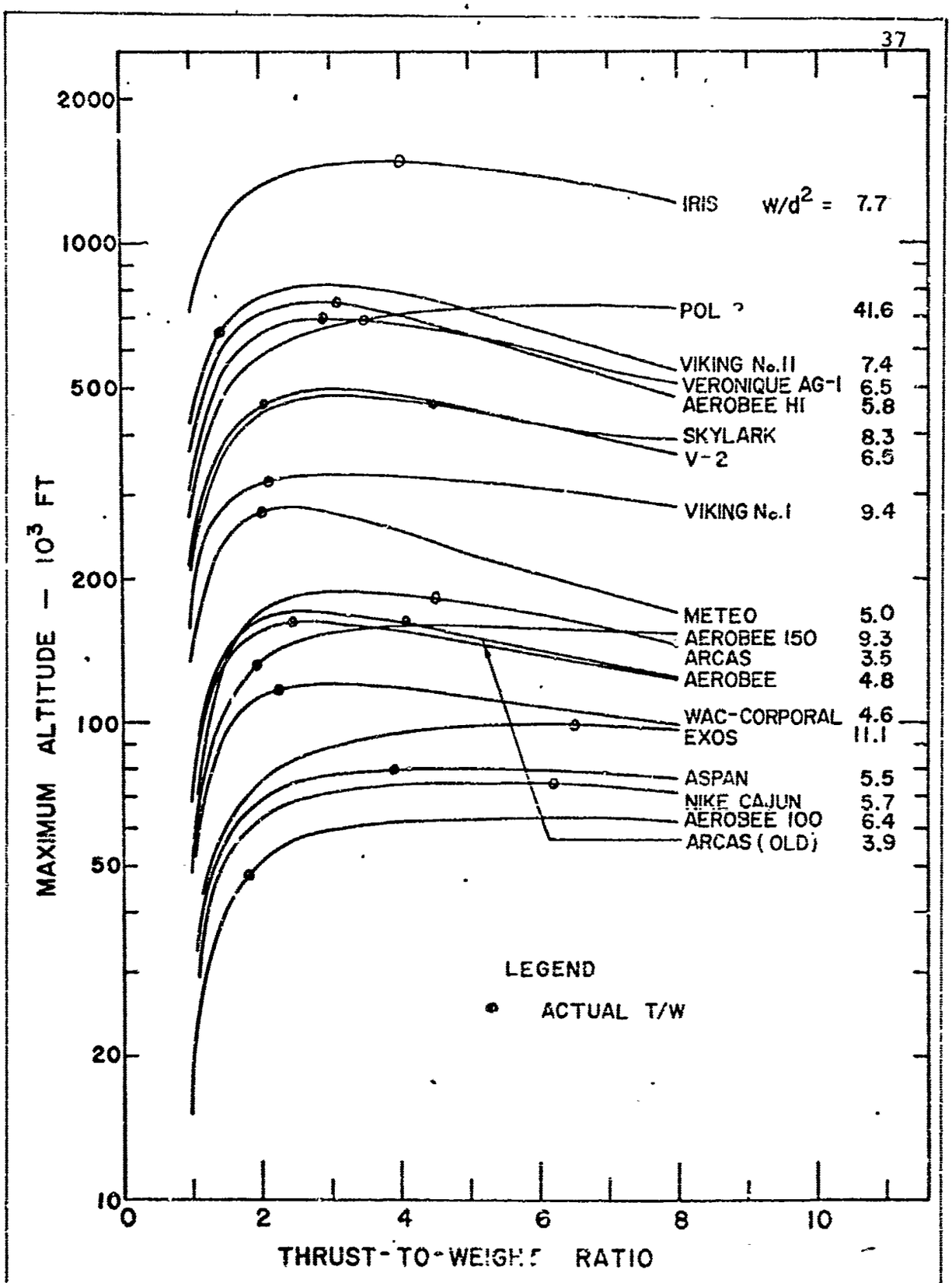

Fig. 4-5. Variations of maximum altitude with thrust-to-weight ratio for real rockets, under simplifying assumptions (pressure thrust neglected, C_D = 0.4, and V_E = ?).

It should be noted that all these rockets were investigated under many simplifying assumptions. Although the calculated maximum altitudes are not valid for their actual performance, yet the location of $(T/W)_{opt}$ is considered reasonably close to that of the real case (See Section 5.3 and Fig. 5-6). It seems that most of the rockets previously investigated were well designed as can be seen from Fig. 4-5. Looking at one particular rocket, the Arcas, which is used extensively for meteorological soundings by the U. S. Army, it is apparent that the present Arcas is an improvement over the older Arcas design. By the preliminary design analysis, it seems, however, that the $(T/W)_{opt}$ of this rocket is lower than the present design T/W. Since, with initial launching velocity, the selection of the optimum T/W becomes critical (Fig. 4-1), it was decided to investigate in more detail the performance of the Arcas.

A preliminary parametric analysis of the performance of Arcas was made under the assumptions used for other rockets in this chapter. The results, regarding the influence of drag coefficient on optimum T/W; and variations of Y_{max}, V_b and Y_b are plotted in Figs. 4-6 and 4-7, respectively. It is apparent that variation in C_D does not alter $(T/W)_{opt}$ significantly, even though Y_{max} would undoubtedly be influenced. This establishes the validity of assuming constant C_D for all rockets in Fig. 4-5 for determining optimum T/W. Figure 4-7 shows that variation of T/W has opposite effect on V_b and Y_b, so that for only one value of $T/W = (T/W)_{opt}$, the Y_{max} is optimized.

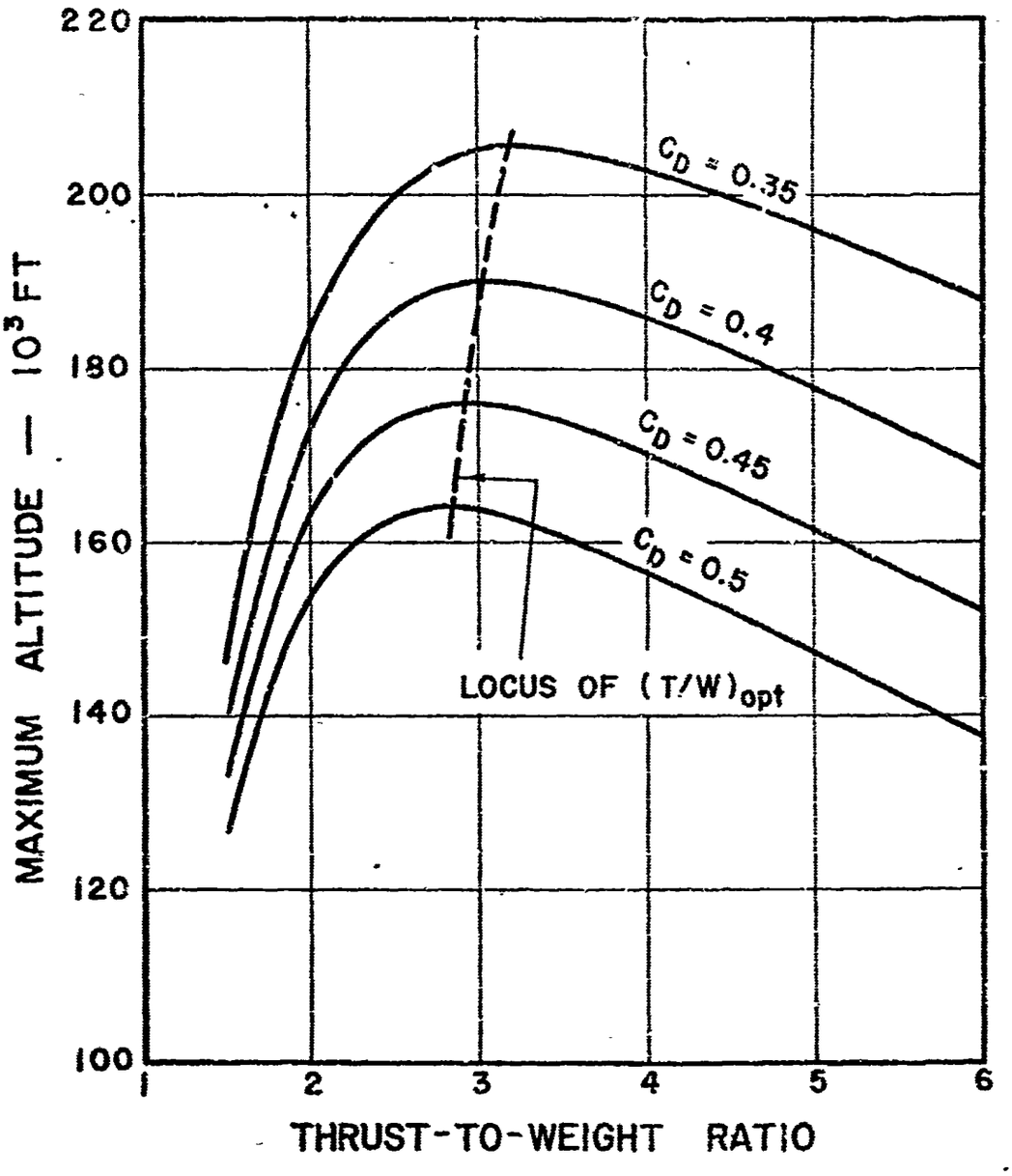

Fig. 4-6. Effect of drag coefficient on optimum thrust-to-weight ratio for the Arcas, under simplifying assumptions (pressure thrust neglected, C_D constant, and $V_0 = 0$).

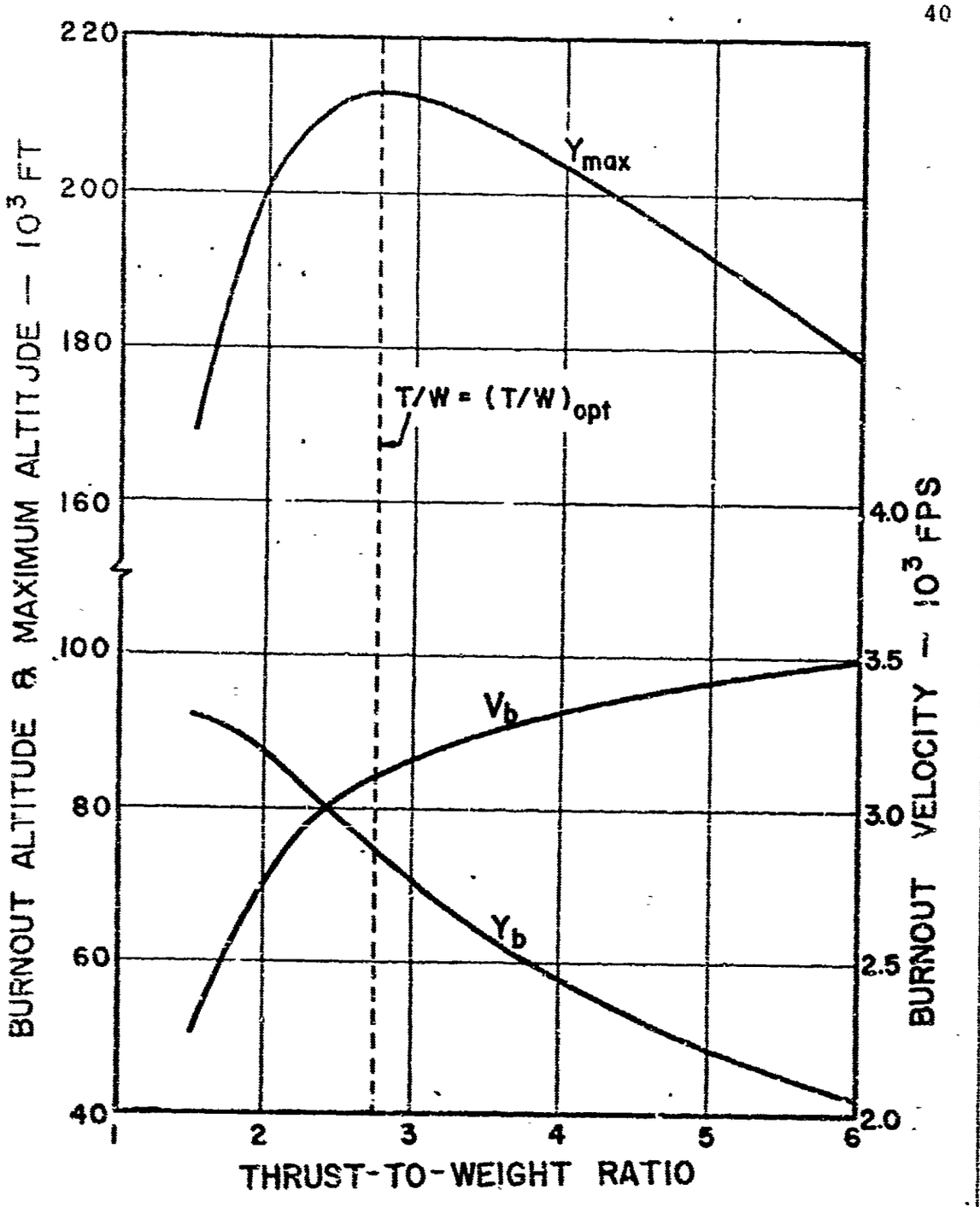

Fig. 4-7. Variations of burnout velocity and burnout altitude with thrust-to-weight ratio for the Arcas, under simplifying assumptions (pressure thrust neglected, $C_D = 0.4$, and $V_0 = 0$).

These plots for Arcas were made for most simplified conditions. A much more accurate analysis of its realistic performance is presented in the next chapter.

CHAPTER V

OPTIMIZATION STUDIES ON THE PERFORMANCE OF THE ARCAS ROCKET

5.1 Introductory Comments

The Arcas (All Purpose Rocket for Collecting Atmospheric Soundings) was developed for the office of Naval Research by the Atlantic Research Corporation. Work commenced on this project in January 1958, and by July of the same year a successful test firing was made from Wallops Island. Further testing was accomplished by the Army Signal Corps at White Sands Missile Range, New Mexico, in early 1959. Development of this rocket has been continuing since then.

The Arcas is designed to collect meterological data at altitudes up to 40 miles and thus aid in constructing routine weather forecasts. It is propelled by a single solid-rocket motor with a cigarette-end slow-burning propellant. The Arcas, which weighs only 70 lb, is designed to replace the expensive two-stage rockets like Aerobee and Nike-Cajun, which are many times as expensive and have been used extensively in the past to gather weather data. The Arcas is now a current meteorological sounding rocket of the U. S. Army. In the preliminary

analysis (Chapter IV), it was found that the present design T/W of the Arcas seems to be higher than its optimum value. Since, with an initial launching velocity, the selection of the optimum T/W becomes critical, it is considered necessary to investigate its performance in more detail.

In this optimization study, the thrust-to-weight ratio is varied by changing the propellant flow rate in the nozzle. This is controlled by modifying the nozzle size and the exposed burning surface of the grain. The geometrical configuration of the nozzle, however, is maintained unchanged. Other parameters such as specific impulse, fuel ratio, lift-off weight, dimaeter and chamber pressure are also assumed to remain the same.

The effects of the pressure thrust due to variations of atmospheric pressure with altitude, and variable drag coefficient as a function of Mach number may have been included in this study. Thus, this analysis provides a reasonably good analytical simulation of the estimated real performance of Arcas.

5.2 Characteristics of Arcas

Data for the present Arcas as obtained around January 1969 from Dr. Louis Duncan of the White Sands Missile Range, New Mexico, are listed below:

i) Lift-off weight, W = 70 lb.

ii) Weight of propellant, W_p = 30 lb.

iii) Diameter, d = 4.45 in.

iv) Effective area of nozzle exit, A_e = 2.55 sq. in.

v) Propellant flow rate, $\dot{w}$ = 1 lb_m/sec.

vi) Total thrust, T, is calculated as follows:

$$T = T_{SL} + A_e(P_{SL} - P_a)$$

in which the experimental data for sea-level thrust history is shown in Fig. 5-1.

vii) Experimental data for variations of drag coefficient with Mach number during burn phase and during power-off are shown in Fig. 5-2.

From these data, the average sea-level thrust, $\bar{T}_{SL}$, is found to be 315 lb. Thus, T/W = 4.5 and I_{sp} = 315 sec.

Change in thrust-to-weight ratio results in a corresponding change in flow rate and burning time. Accordingly, a modified sea-level thrust history is to be expected. The sea-level thrust history of the present Arcas (Fig. 5-1) is nondimensionalized in the form $T_{SL}/\bar{T}_{SL}$ versus t/t_b as shown in Fig. 5-3.

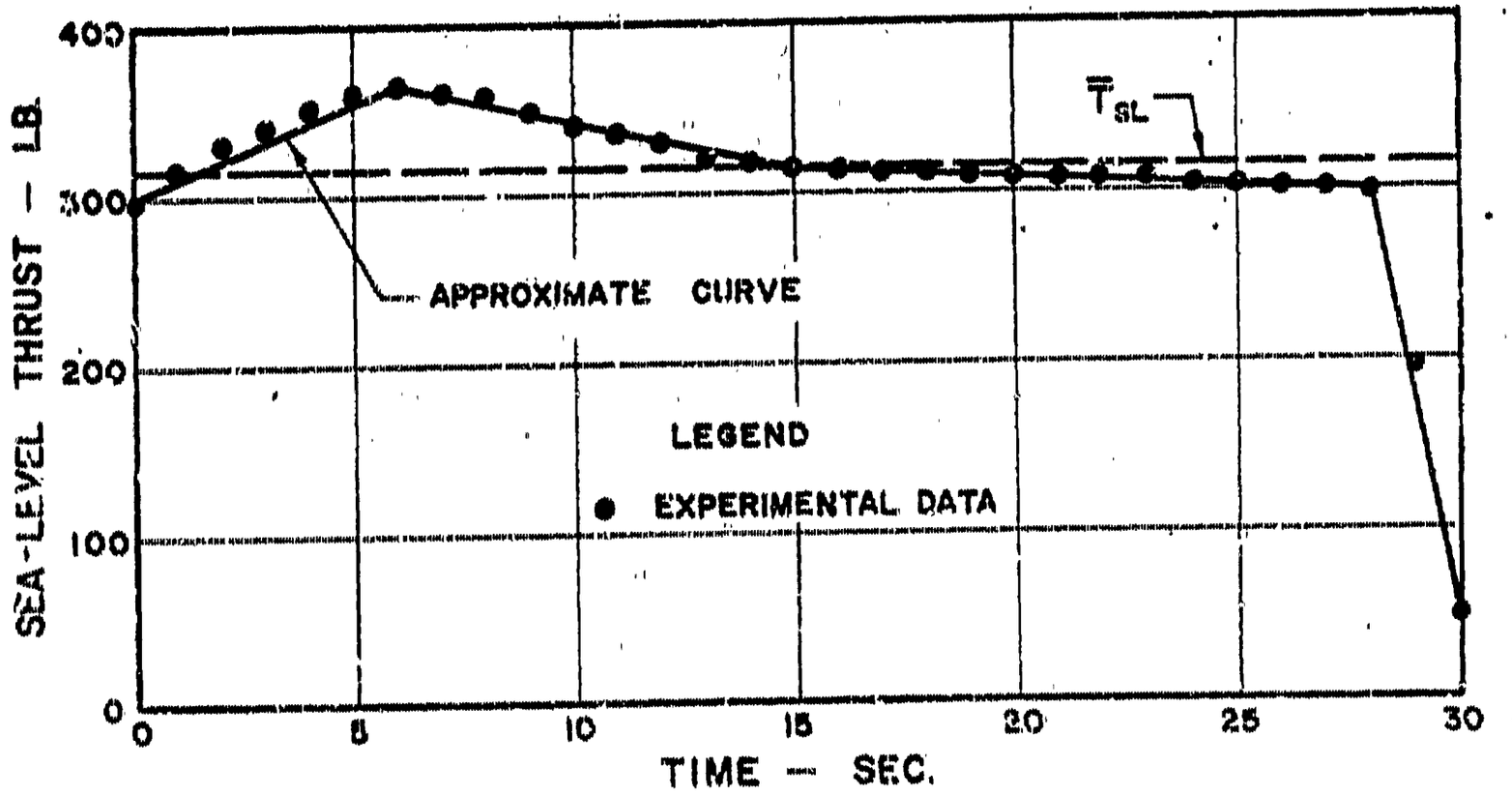

Fig. 5-1. Experimental sea-level thrust history for the present Aerex.

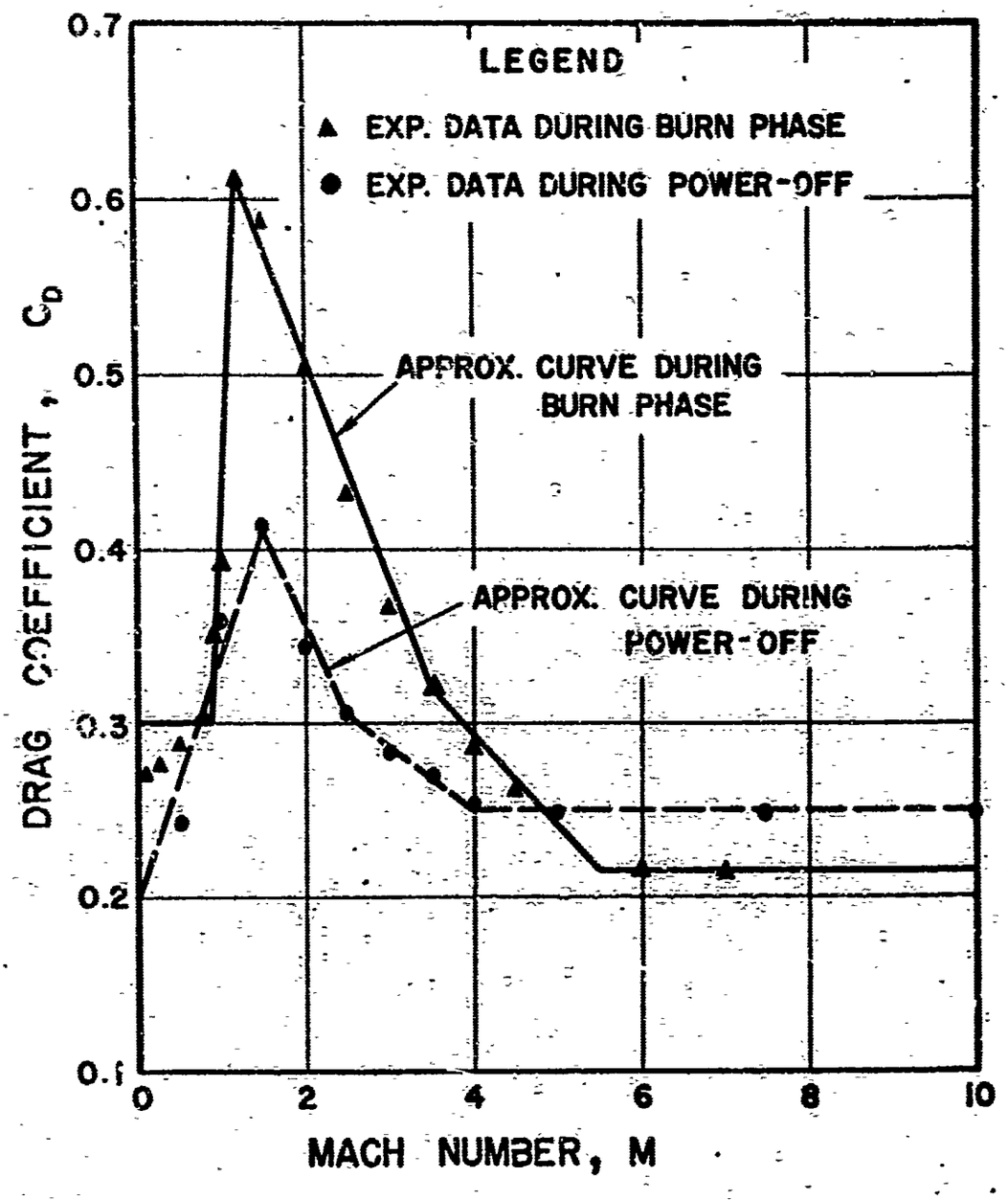

Fig. 5-2. Variations of drag coefficient with Mach number for the present Arcas.

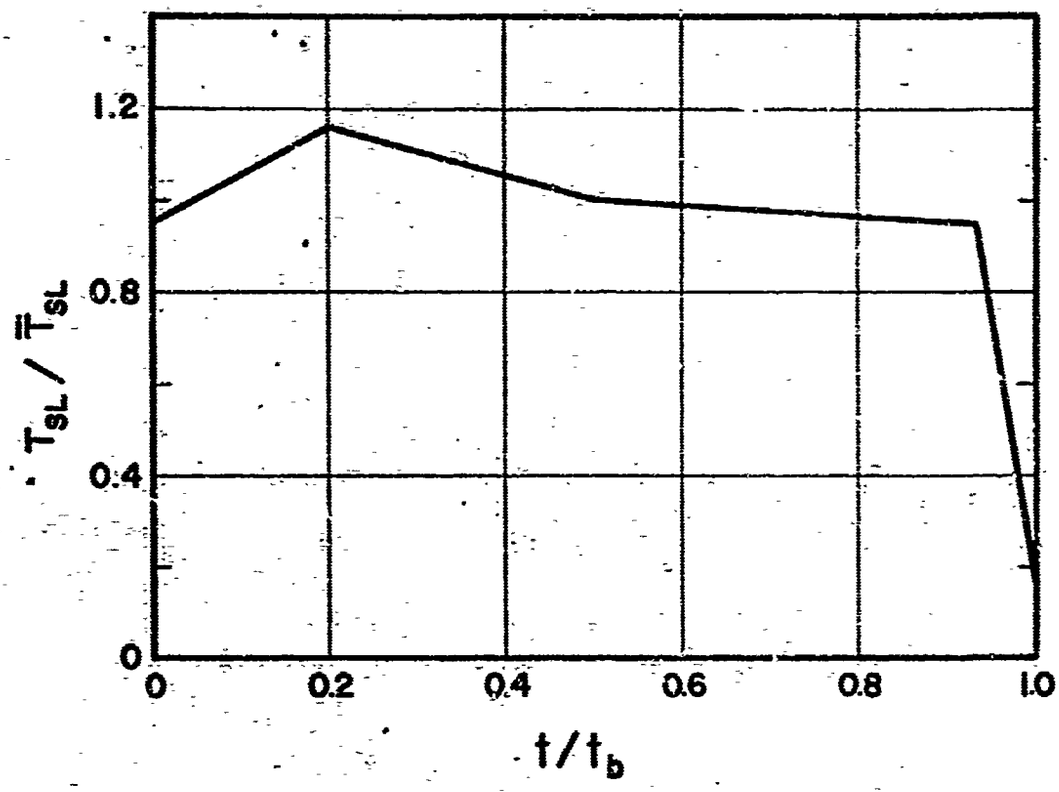

Fig. 5-3. Non-dimensionalized sea-level thrust history for the Arcas, based on the present Arcas data.

This non-dimensionalized sea-level thrust history is considered valid for other thrust-to-weight ratios and is expressed in the following simple equations:

$$T_{SL} = \overline{T}_{SL} \ (0.953 + 1.03 \ t/t_b)$$

for $0 \leq t/t_b \leq 0.2$,

$$T_{SL} = \overline{T}_{SL} \ (1.265 - 0.53 \ t/t_b)$$

for $0.2 < t/t_b \leq 0.5$,

$$T_{SL} = \overline{T}_{SL} \ (1.0543 - 0.1086 \ t/t_b)$$

for $0.5 < t/t_b \leq 0.933$, and

$$T_{SL} = \overline{T}_{SL} \ (12.059 - 11.9 \ t/t_b)$$

for $0.933 < t/t_b \leq 1$,

in which, $\overline{T}_{SL}$ is the average sea-level thrust and is given by the product of propellant flow rate (in lb_m/sec) and specific impulse.

The C_D curves during burn phase and during power-off, based on the data obtained from White Sands, are closely approximated by a number of straight lines as shown in Fig. 5-2 and given by simple equation as follows:

i) During burn phase

C_D .. for $M < 0.9$,

$C_D = 0.3 + 1.073\ (M - 0.9)$ for $0.9 \leq M < 1.2$,

$C_D = 0.321 + 0.1309\ (3.5 - M)$ for $1.2 \leq M \leq 3.5$,

$C_D = 0.215 + 0.053\ (5.5 - M)$ for $3.5 \leq M \leq 5.5$,

$C_D = 0.215$ for $M > 5.5$.

ii) During power-off

$C_D = 0.2 + 0.1417\ M$ for $M < 1.5$,

$C_D = 0.305 + 0.1075\ (2.5 - M)$ for $1.5 \leq M < 2.5$,

$C_D = 0.25 + 0.0366\ (4 - M)$ for $2.5 \leq M \leq 4$,

$C_D = 0.25$ for $M > 4$.

It is obvious that the C_D curve during burn phase changes with the propellant flow rate. Since the experimental C_D curve is known only for the present Arcas (T/W = 4.5), it is assumed that the increment of C_D due to burning is linearly proportional to the propellant flow rate. Therefore, on the basis of the C_D curve available for the present Arcas, the C_D curve for other thrust-to-weight ratios during burning may be estimated as follows:

$$(C_D)_{T/W} = (C_D)_{\text{power-off}} + \frac{\left[(C_D)_{\text{burn phase}} - (C_D)_{\text{power-off}}\right]_{T/W = 4.5}}{(\dot{w})_{T/W = 4.5}} \times (\dot{w})_{T/W}$$

The approximate expressions for non-dimensionalized sea-level thrust history and C_D curves as discussed above have been derived for computational simplicity.

A change of thrust-to-weight ratio for a rocket may be accomplished by several methods. One of the simple ways of changing T/W for a rocket of the same weight is by merely changing the nozzle size and achieving a corresponding burn rate. Accordingly, it is assumed here that T/W is altered by a change of the nozzle size. Further, another reasonable assumption that is made here is that the area of the nozzle exit is linearly proportional to the propellant flow rate. Based on these considerations, for the present Arcas with $\dot{w}$ = 1 lb_m/sec and A_e = 2.55 sq. in., if T/W is changed, one can readily determine the A_e for any T/W (or a corresponding $\dot{w}$).

5.3 Optimization of the Arcas Rocket

To maximize the obtainable altitude reached by Arcas, the thrust-to-weight ratio is altered by changing its nozzle size and propellant flow rate. This, in turn, changes the sea-level thrust history and the C_D curve during burn phase. On the basis of the information on the present Arcas (T/W = 4.5), the area of nozzle exit, sea-level thrust history and C_D curve during burn phase are estimated for any other T/W as described in Section 5.2. For optimization studies, these estimates will be used here. Furthermore, since the thrust of the rocket not

only includes the momentum thrust due to rocket propulsion but also the pressure thrust due to variations of altitude, this pressure thrust influence has also been included for optimization analysis. The total thrust was thus calculated by the previously mentioned relation

$$T = T_{SL} + A_e (P_{SL} - P_a)$$

Numerical integrations of the equations of motion, including the variations of the thrust and the drag coefficient, were carried out to solve the maximum altitudes for T/W in the range of 1 to 6 with initial velocities of 0, 200, 400, 600, 800 and 1,000 fps respectively. Plots of Y_{max} versus T/W for different initial velocities are presented in Fig. 5-4.

The following observations may be made from Fig. 5-4:

i) The optimum thrust-to-weight ratios are practically identical for different initial velocities,

$$(T/W)_{opt} \approx 2.4.$$

ii) For $T/W < 2$, the performance of Arcas, in terms of Y_{max}, is degraded quite steeply.

iii) For $T/W > (T/W)_{opt}$, Y_{max} decreases nearly linearly with increasing T/W. Its slope increases only slightly with increasing initial velocity.

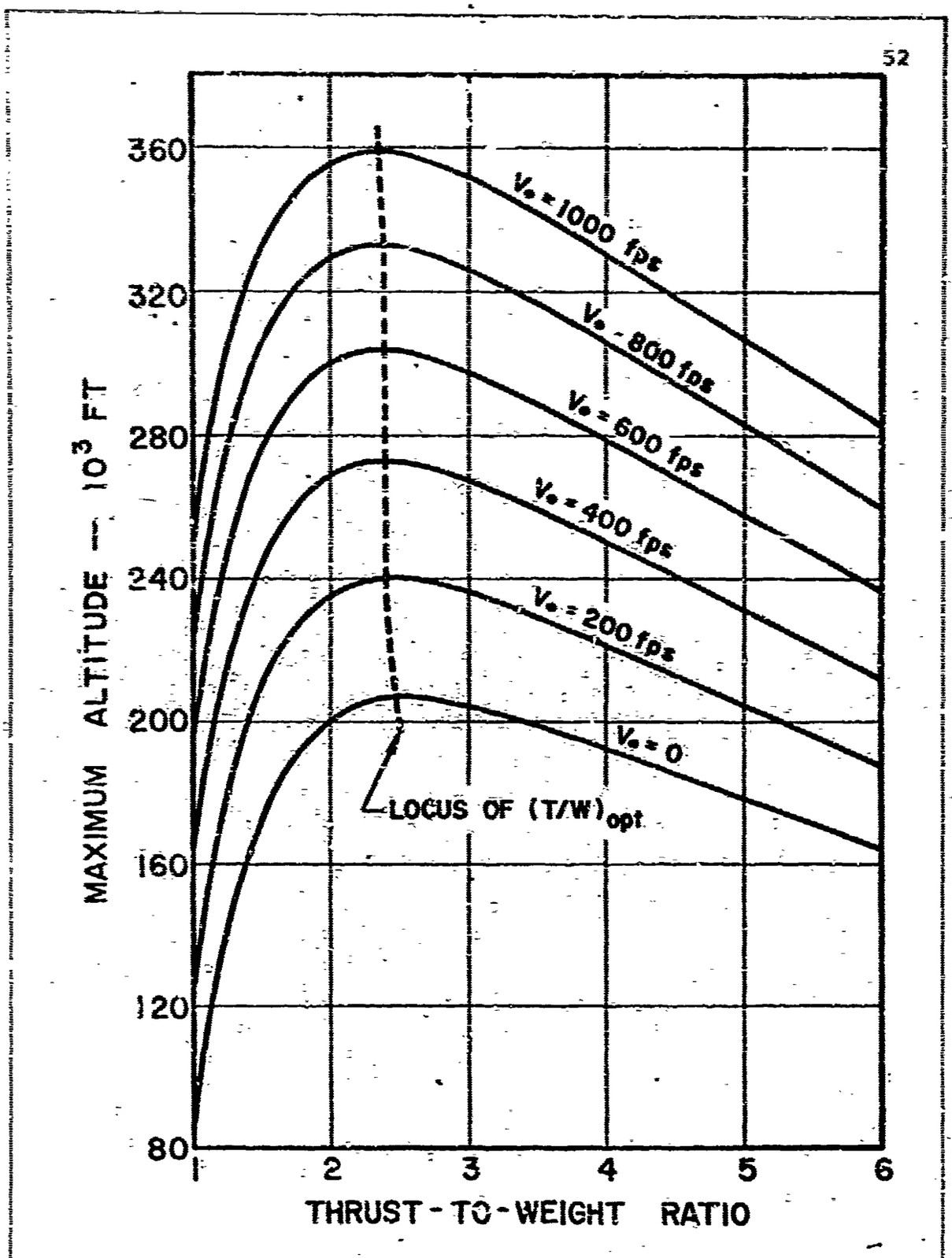

Fig. 5-4. Variations of maximum altitude with thrust-to-weight ratio for the Arcas (estimated realistic performance).

iv) For each initial velocity, about 13 per cent increase in Y_{max} is obtained when T/W is altered from the present design value of 4.5 to 2.4, which is determined by this analysis as the desired optimum T/W for the Arcas rocket.

v) The gain in Y_{max} due to the initial velocity, imparted by the VAMB system, is very significant. For instance, 73 per cent increase in Y_{max} is obtained by imparting an initial velocity of 1,000 fps when $T/W = (T/W)_{opt}$.

The burnout velocities and burnout altitudes for different initial velocities when $T/W = (T/W)_{opt}$ and T/W = 4.5, are given in Table 5-1.

The integrated drag, Q, throughout the flight is a measure of the total energy loss due to aerodynamic drag. Figure 5-5 shows that the Q increases with the initial velocity. However, the percentage increase in Q (for T/W = 2.4) due to initial velocity up to 600 fps is only 6.5 per cent or less. It is 19 per cent for initial velocity of 1,000 fps. Thus, we conclude that the increase in the integrated drag loss due to the imparted initial velocity up to 600 fps, is almost negligible.

It should be noted that all the computations for the realistic performance estimates of Arcas as given in Figs. 5-4 and 5-6 are still based on certain postulations. For defining the present optimization problem, the gross weight, payload, structural weight, the propellant weight and its specific impulse have all been maintained unchanged for the Arcas rocket. These postulations were felt necessary to make the present aerodynamic performance optimization study tractable. However, for a real design study, variations in structural requirements and propulsion

Table 5-1. Estimates of burnout velocities, burnout altitudes and maximum altitudes for the proposed optimized and the present Arcas (Section 5.2), both launched from sea-level conditions.

Initial velocity imparted	Proposed optimized Arcas (T/W = 2.4) performance			Estimates for present Arcas (T/W = 4.5) performance		
V_i fps	V_b fps	Y_b ft	Y_{max} ft	V_b fps	Y_b ft	Y_{max} ft
0	2,920	79,000	206,800	3,200	49,900	185,600
200	3,160	88,300	240,600	3,400	54,500	213,000
400	3,340	97,000	273,200	3,600	58,800	240,600
600	3,590	105,000	304,100	3,790	63,000	267,900
800	3,770	113,000	333,100	3,950	67,000	294,500
1,000	3,920	120,000	338,900	4,110	70,600	319,200

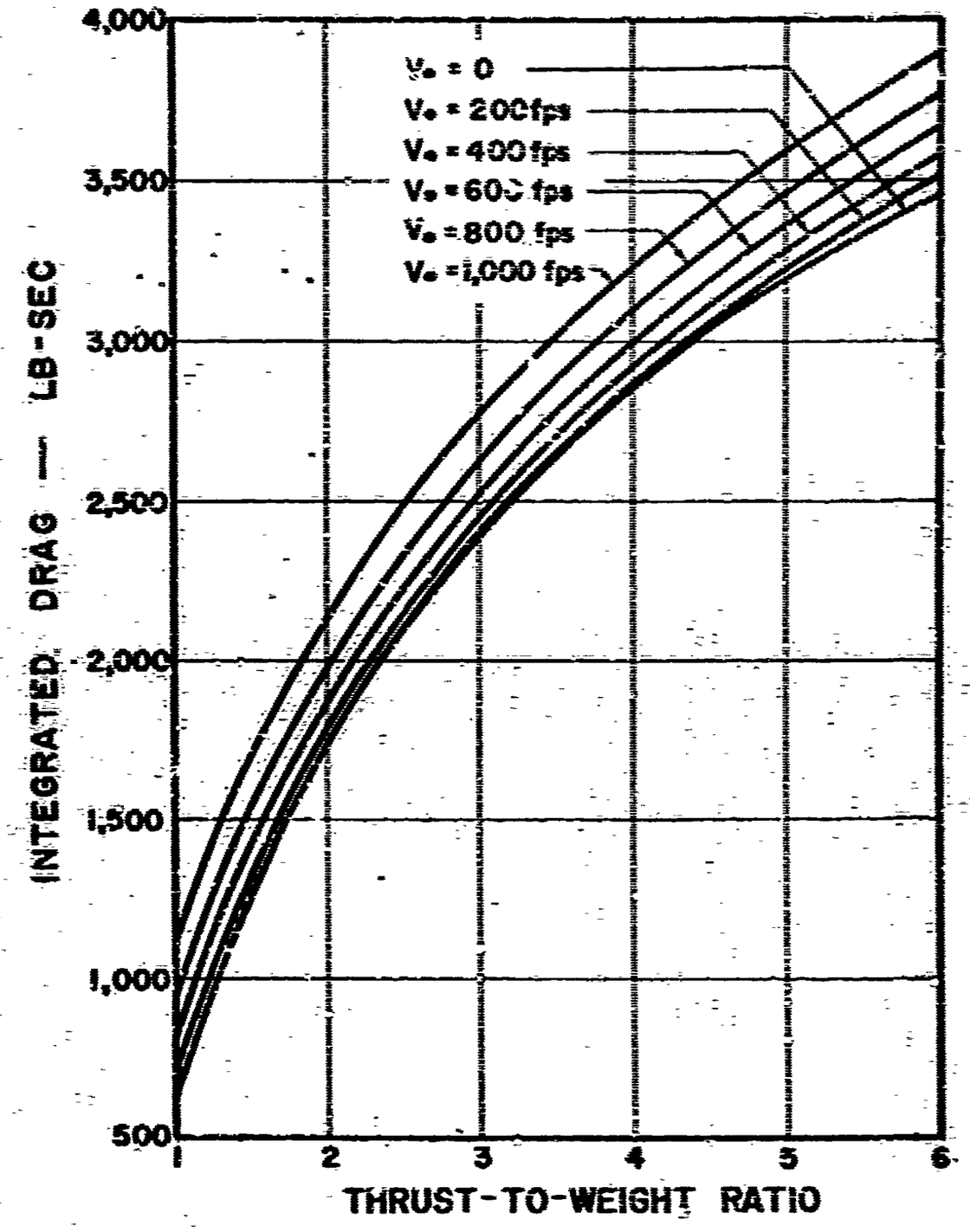

Fig. 5-5. Variations of integrated drag with thrust-to-weight ratio for the Arcas (estimated realistic performance)

plant design (e.g., chemical characters of the propellant, burning surface alterations and nozzle variations) should also be included. It was not possible to incorporate these considerations in the present study. It is felt, however, that the aerodynamic design optimization procedure as developed here is an important first step towards accomplishing a final optimized design.

The performance analysis computations made for Fig. 5-4 were reasonably involved and complicated. For this reason, it may be desirable to evolve a somewhat simpler though less accurate method of performance estimation. Such a method would be of help in a preliminary design study. When the final design, which includes the structural and propulsion considerations, has been firmed up, the more accurate analysis developed above may be used for real performance estimation. With this in mind, computations for Arcas have been made with three cases under different simplifying assumptions, to see which one is the closest to the real performance case. These three simplifying cases are:

a) Thrust constant throughout burn phase and C_D varied.

b) Thrust constant throughout burn phase and C_D constant ($C_D = 0.43$).

c) Thrust (neglecting pressure thrust) constant throughout burn phase and C_D constant ($C_D = 0.43$).

In cases (a) and (b), the pressure thrust is estimated in advance and then added to the momentum thrust. Since it was found that the atmospheric pressure decreases approximately linearly with time during burn phase, the pressure thrust, $A_e (P_{SL} - P_a)$, thus also increases linearly with time approximately.

Once the burnout altitude is known, the ambient atmospheric pressure at this altitude is determined. And the average pressure thrust can then be estimated. Plots of Y_{max} versus T/W for cases (a), (b), (c) along with the actual performance as presented in Fig. 5-4, are given in Fig. 5-6 for comparative purposes.

In case (a), $(T/W)_{opt} \approx 2.6$. In case (b), $(T/W)_{opt} \approx 2.8$. In case (c), $(T/W)_{opt} \approx 2.8$. The $(T/W)_{opt}$ value is interestingly not altered much for any of these cases. Thus, for preliminary design considerations, to select the most desirable T/W, it is considered feasible to achieve this by the simplest of these methods, represented by case (c); i.e., when both thrust and drag coefficients are constant and the pressure thrust is also neglected. This approach was used to determine the optimum T/W for over a dozen different rockets discussed earlier (Fig. 4-5). Results of that analysis regarding optimum T/W are therefore considered valid.

For estimation of Y_{max}, however, case (c) is not suitable. For Arcas, the error in Y_{max} in this case is approximately 14 per cent. This error is primarily due to the neglect of the pressure thrust. It seems, therefore, that the contribution of pressure thrust to Y_{max} is quite significant even though the pressure thrust itself is only a few per cent of the momentum thrust.

Therefore, for reasonably close estimations of both $(T/W)_{opt}$ and Y_{max}, case (b) is considered suitable. It does require, however, that the designer choose the constant C_D and constant thrust quite intelligently. Estimation of the pressure

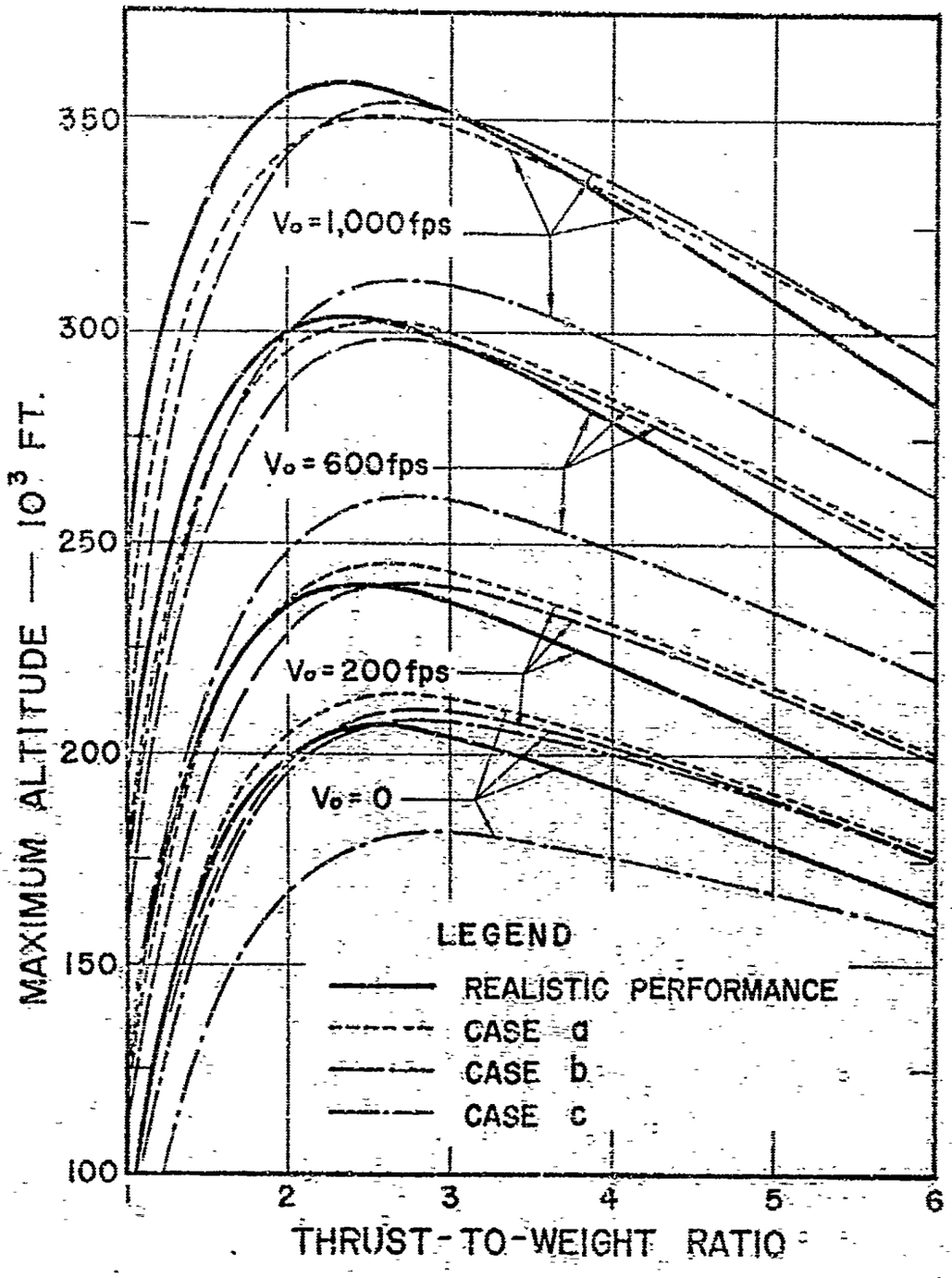

Fig. 5-6. Comparisons of three simplifying cases:

(a) constant thrust and varied C_D,
(b) constant thrust and constant C_D,
(c) constant thrust (neglecting pressure thrust) and constant C_D, with estimated realistic performance of Arcas.

thrust contribution can be made readily for rockets which have a burnout altitude of 60,000 ft or more. Since, above this altitude the ambient atmospheric pressure is less than 7 per cent of the atmospheric pressure at sea-level, the pressure thrust term can be estimated on the assumption that the ambient atmospheric pressure at burnout is zero. As discussed before, the variation of pressure thrust term, $A_e (P_{SL} - P_a)$, is nearly linear with time. So, a good approximation for including the pressure thrust contribution for case (b) will be to include the term $A_e (P_{SL}/2)$ along with the assumed constant momentum thrust for the whole duration of the powered flight.

5.4 Stagnation Temperature and Pressure

Missile or aircraft flights at high speeds and high altitudes introduce many new problems to the designer. One of the more important problems that arises is caused by the skin temperatures (aerodynamic heating) that are attained at very high velocities. Adiabatic wall temperatures under these conditions can exceed temperature limitations of structural materials commonly used in the manufacture of such missiles. Although the maximum velocity of the Arcas is not greater than 4,000 fps, it is still considered necessary to have the information concerning the stagnation temperatures.

The stagnation temperature, defined as the total temperature of the gas at rest, is:

$$T_0 = T_a + V^2/2C_p$$

Where

T_0 = stagnation temperature,

T_a = ambient temperature,

V = free-stream velocity,

C_p = specific heat at constant pressure.

It is known that C_p is not significantly affected by temperature and may be assumed to be a constant. For air, it is assumed that $C_p = 0.25$.

Stagnation temperatures for the Arcas during optimum performance as computed from the above relation are shown in Fig. 5-7 and the maximum values for different initial velocities are l. ! in Table 5-2.

It should be indicated that the maximum stagnation temperature is reduced when the T/W is altered from its present design value (T/W = 4.5) to that of the proposed optimum case (T/W = 2.4). In fact, for initial velocities of nearly 500 fps, the maximum stagnation temperature for the optimized case is below the maximum stagnation temperature for the present Arcas. Even with an initial velocity of 1,000 fps, this temperature for the optimum case is only 1,680 ^{o}R which can be readily withstood by the present nosecone materials. Similarly, the external skin temperatures are expected to be within reasonable design limits.

It can thus be concluded that the aerodynamic heating of Arcas due to impartation of initial velocity is no problem for existing designs.

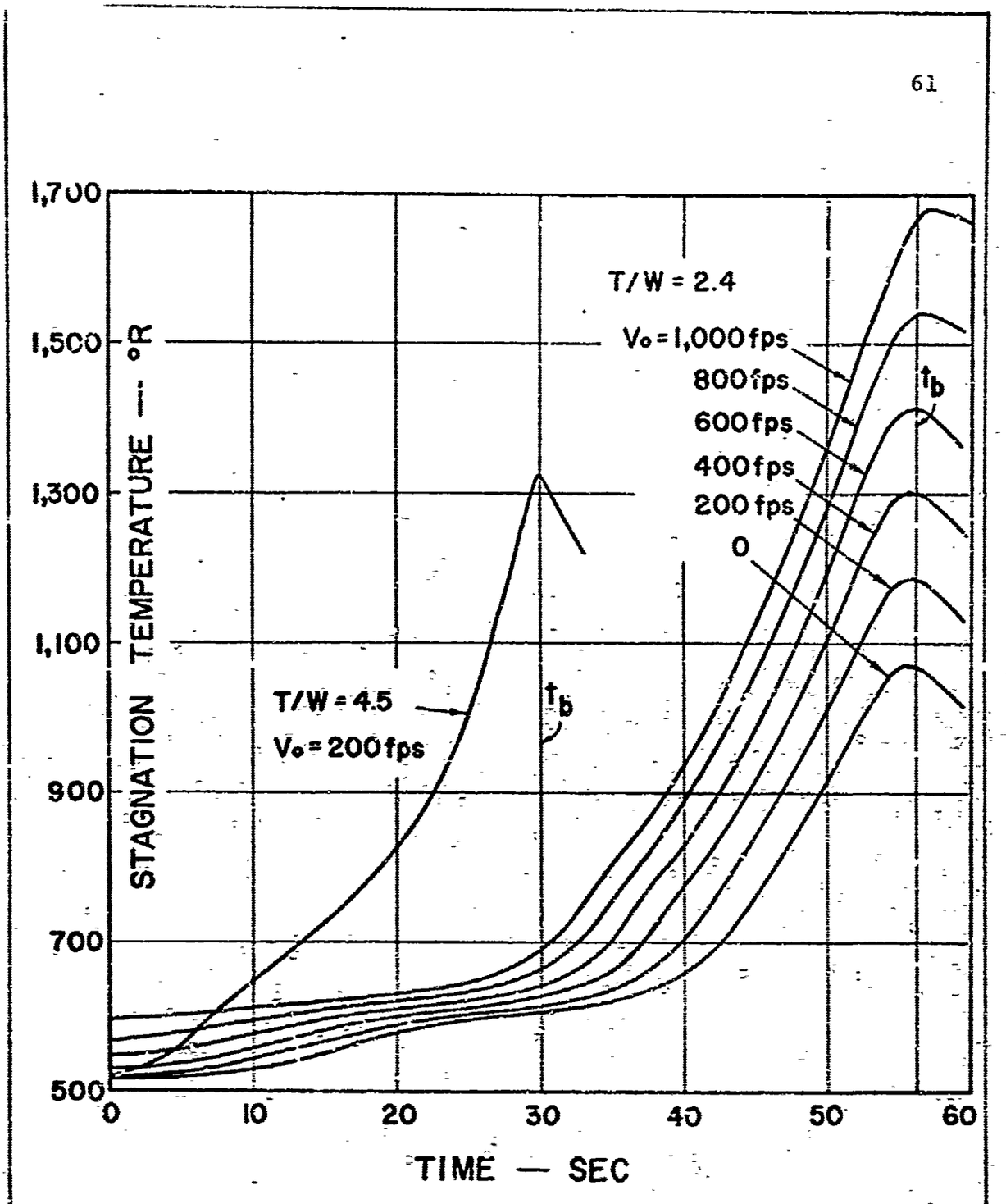

Fig. 5-7. Stagnation temperatures for the Arcas during powered flight when $T/W = (T/W)_{opt}$ and $T/W = 4.5$.

Table 5-2. Maximum stagnation temperatures for the proposed optimized and the present Arcas.

	T/W	V_0 fps	$(T_0)_{max}$ °R
Proposed optimized Arcas	2.4	200	1,190
	2.4	400	1,300
	2.4	600	1,420
	2.4	800	1,540
	2.4	1,000	1,680
Present Arcas	4.5	200	1,320

The stagnation pressure, defined as the sum of the ambient and the dynamic pressures, is given by

$$P_0 = P_a + \rho V^2/2$$

where

P_0 = stagnation pressure,

P_a = ambient pressure,

ρ = ambient density,

V = free stream velocity.

Variations in stagnation pressure during powered flight for the present Arcas and for the proposed optimized Arcas are presented in Fig. 5-8. It can be seen that the maximum stagnation pressure is reduced from 25 psi to 16 psi when the T/W is altered from its present design value to the proposed optimum value. Even with an imparted initial velocity of 1,000 fps, the maximum stagnation pressure (23 psi) for the optimum case is still lower than for the present Arcas. This is well within the existing design limits and thus represents no problems.

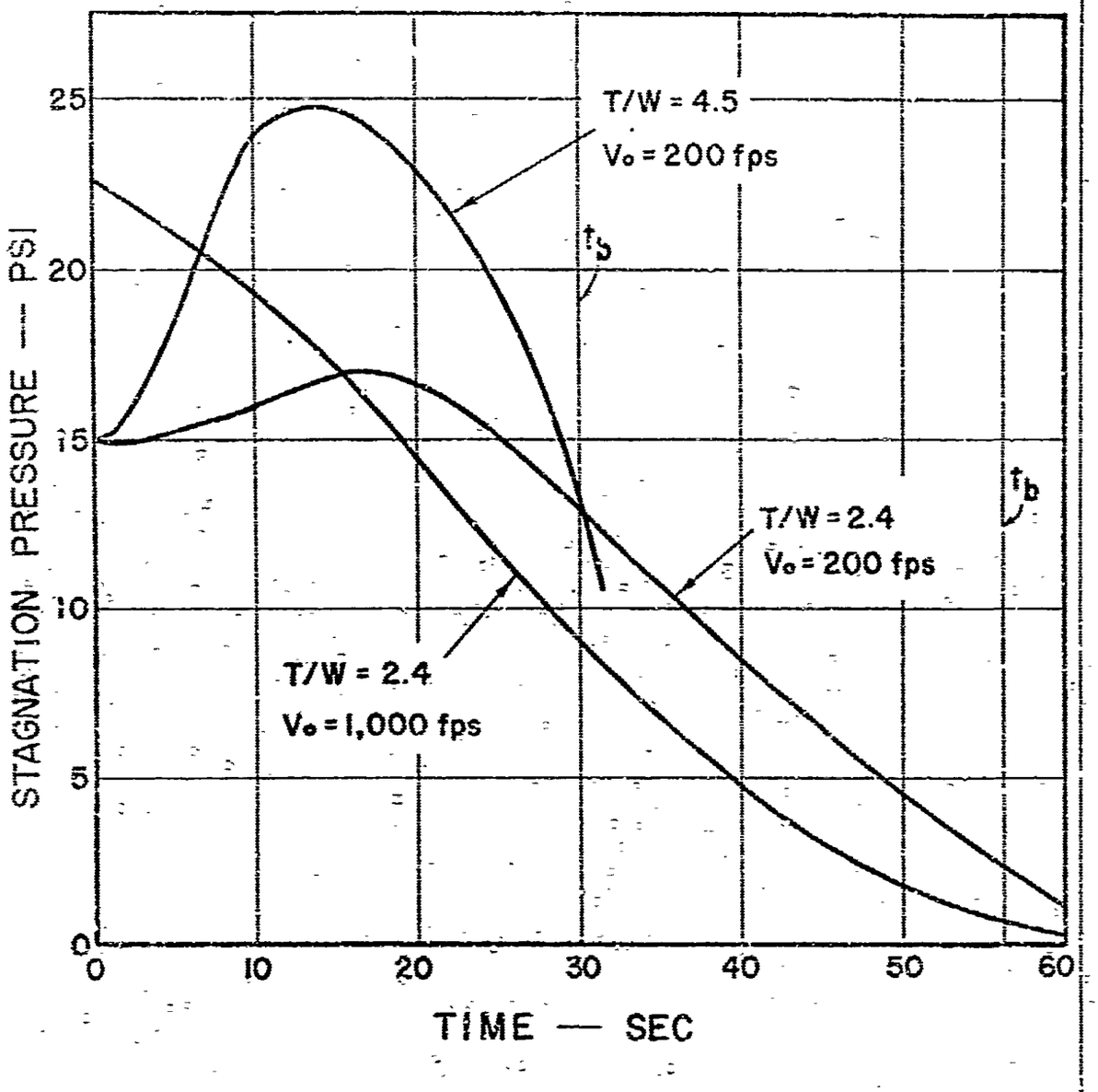

Fig. 5-8. Stagnation pressures for the Arcas during powered flight when $T/W = (T/W)_{opt}$ and $T/W = 4.5$.

CHAPTER VI

CONCLUSIONS AND SUGGESTIONS FOR FUTURE WORK

Significant gains in performance of single-stage rockets are considered possible by utilizing the VAMB system. The gain in maximum altitude of an optimized Arcas when launched with an initial velocity of 1,000 fps is expected to be 93 per cent above the estimated maximum altitude of the present design Arcas without booster. Comparable gains for other single-stage rockets are also expected. It seems that single-stage rockets designed in an optimum fashion for conventional launch will continue to perform near optimum even with the VAMB system. This was found to be the case for Arcas. For other rockets, however, a similar optimization study should be performed. It is felt that beyond the aerodynamic optimization as presented in this thesis, an integrated optimization study, for the individual rocket, including the structural and propulsion design variations, should be performed to evolve the final optimum design.

It is feasible, for preliminary optimization study, to assume that both thrust and coefficient of drag are constant and the pressure thrust is negligible. The estimation of optimum

T/W under this assumption is reasonably valid (Fig. 5-6). This approach was used to determine the optimum T/W for nearly twenty rockets (see Section 4.3).

However, for reasonably close estimations of both $(T/W)_{opt}$ and Y_{max}, the estimated average pressure thrust should also be included. In this case, it is imperative that the constant thrust and constant drag coefficient be intelligently chosen. As a good first approximation, the average pressure thrust can be estimated to be $A_e\ (P_{SL}/2)$.

The selection of T/W is particularly important for rockets having high initial velocity, low $W/C_D d^2$ value and fuel ratio approaching unity. For most rockets, their performance degrades drastically when $T/W < 2$.

The optimum T/W of a small single-stage rocket does not seem to vary with the imparted initial velocity. For Arcas, its $(T/W)_{opt}$ seems to be around 2.4 for $0 < V_0 < 1{,}000$ fps.

The total energy loss due to aerodynamic drag is not increased significantly by imparting an initial velocity. For the optimized Arcas, this increase is 6.5 per cent or less for initial velocities up to 600 fps. It is 19 per cent for V_0 = 1,000 fps.

This study is essentially concerned with the aerodynamic performance optimization. It does not include variations in structural requirements and propulsion plant design. It is recommended that these considerations be incorporated with the aerodynamic performance analysis developed here to accomplish the final optimum design. Optimization of a multi-stage rocket based on the approach developed here should also be undertaken.

APÊNDICE

PROGRAM 1

```
      LEAST SQUARES CURVE FIT FOR VARIATION OF ATMOSPHERIC DENSITY
      WITH ALTITUDE


      DIMENSION A(3,3),B(3),Y(20),RHO(20),RHOC(20),Z(20)
      READ(1,1) K,N
    1 FORMAT(2I2)
      READ(1,2) (Y(I),RHO(I),I=1,K)
    2 FORMAT(2F10.0)
      A(1,2)=0.
      A(1,3)=0.
      A(2,3)=0.
      A(3,3)=0.
      B(1)=0.
      B(2)=0.
      B(3)=0.
      DO 10 I=1,12
      A(1,2)=A(1,2)+Y(I)
      A(1,3)=A(1,3)+Y(I)**2
      A(2,3)=A(2,3)+Y(I)**3
      A(3,3)=A(3,3)+Y(I)**4
      B(1)=B(1)+RHO(I)
      B(2)=B(2)+RHO(I)*Y(I)
      B(3)=B(3)+RHO(I)*Y(I)**2
   10 CONTINUE
      A(1,1)=12.
      A(2,1)=A(1,2)
      A(2,2)=A(1,3)
      A(3,1)=A(1,3)
      A(3,2)=A(2,3)
      CALL SIMQ(A,B,N,N,KS)
      IF(KS) 30,11,30
   11 WRITE(3,12) B(1),B(2),B(3)
   12 FORMAT(1H1,2X,3HB1=,E16.8,5X,3HB2=,E16.8,5X,3HB3=,E16.8)
      WRITE(3,13)
   13 FORMAT(10X,8HALTITUDE,10X,10HACTUAL RHO,10X,15HAPPROXIMATE RHO)
      DO 20 I=1,12
      RHOC(I)=B(1)+B(2)*Y(I)+B(3)*Y(I)**2
   20 WRITE(3,21) Y(I),RHO(I),RHOC(I)
   21 FORMAT(8X,F10.1,8X,E16.8,6X,E16.8)
      SUMY=0.
      SUMZ=0.
      SUMYZ=0.
      SUMY2=0.
      DO 15 I=12,K
      Z(I)=ALOG10(RHO(I))
```

```
      SUMY=SUMY+Y(I)
      SUMZ=SUMZ+Z(I)
      SUMYZ=SUMYZ+Y(I)*Z(I)
   15 SUMY2=SUMY2+Y(I)**2
      D=FLOAT(9)*SUMY2-SUMY**2
      DA=SUMZ*SUMY2-SUMY*SUMYZ
      DC=FLOAT(9)*SUMYZ-SUMY*SUMZ
      P=10.**(DA/D)
      C=DC/D/ALOG10(2.718)
      DO 25 I=12,K
      RHOC(I)=P*EXP(C*Y(I))
   25 WRITE(3,26) Y(I),RHO(I),RHOC(I)
   26 FORMAT(8X,F10.1,8X,E16.8,6X,E16.8)
      WRITE(3,27) P,C
   27 FORMAT(1X,2HP=,E16.8,5X,2HC=,E16.8)
   30 STOP
      END
$DATA

      20 3

      0.          0.07647
      5000.       0.06590
      10000.      0.05648
      15000.      0.04814
      20000.      0.04077
      25000.      0.03431
      30000.       .02866
      35000.      0.02375
      40000.      0.01890
      45000.      0.01487
      50000.      0.01171
      55000.      0.00922
      60000.      0.00726
      65000.      0.00572
      70000.      0.00448
      75000.      0.00351
      80000.      0.00276
      85000.      0.00217
      90000.      0.00171
      100000.     0.00107
```

PROGRAM 2

```
      NUMERICAL SOLUTION OF THE EQUATION OF MOTION FOR A VERTICAL
      TRAJECTORY


      DIMENSION Y(2),DERY(2),YN(2),YNN(2),YNNN(2)
      COMMON AREA,CD,RHO1,ALPHA,    WFR,WF,BRATE,BT,G,A,B,C,ANUM,  RHO
     1       ,AMACH,TINF,A1,B1,C1,P1,ALPHA1,THAV,P
      RHO1=0.129184
      ALPHA=-0.480263E-4
      A=0.757878E-1
      B=-0.203365E-5
      C=0.150855E-10
      P1=0.265263E4
      ALPHA1=-0.473109E-4
      A1=0.20839SE4
      B1=-0.666794E-1
      C1=0.596168E-6
      G=32.2
      DT=0.5
  100 READ(1,9) WFR,D,SPIM,WF
    9 FORMAT(4F10.0)
      VEXH=SPIM*G
      AREA=0.7854*D*D/144.
      FRATIO=WF/WFR
      VZERO=0.
      DO 40 J=1,6
      TW=1.
      DO 50 I=1,11
      THAV=TW*WFR
      BRATE=TW*G*WFR/VEXH
      BT=WF/BRATE
      Y(1)=VZERO
      Y(2)=0.
      T=0.
      WRITE(3,1)
    1 FORMAT(1///,2X,10HTHRUST/WT.,2X,6HFRATIO,2X,9HTOTAL WT.,2X,4HFUEL,
     18X,5HBRATE,4X,5HBTIME,5X,7HEXHVEL.,14X,4HAREA,5X,5HVZERO)
      WRITE(3,2) TW,FRATIO,WFR,WF,BRATE,BT,VEXH,   AREA,VZERO
    2 FORMAT(1H0,7F10.3,10X,2F10.3)
      WRITE(3,3)
    3 FORMAT(1H0,5X,10HTIME(SECS),5X,16HVELOCITY(FT/SEC),5X,
     112HALTITUDE(FT),3X,10HDRAG COEF.      12X,5HDRAGF)
      DRAGF=0.
    4 CALL FCT(T,Y,DERY)
      DRAGF=DRAGF+ANUM*DT/G
      R1=DERY(1)*DT
```

```
      S1=DERY(2)*DT
      TN=T+DT/2.
      YN(1)=Y(1)+R1/2.
      YN(2)=Y(2)+S1/2.
      IF(YN(1).LT.0..AND.Y(2).GT.0.) GO TO 21
      CALL FCT(TN,YN,DERY)
      R2=DERY(1)*DT
      S2=DERY(2)*DT
      YNN(1)=Y(1)+R2/2.
      YNN(2)=Y(2)+S2/2.
      IF(YNN(1).LT.0..AND.Y(2).GT.0.) GO TO 21
      CALL FCT(TN,YNN,DERY)
      R3=DERY(1)*DT
      S3=DERY(2)*DT
      TNN=T+DT
      YNNN(1)=Y(1)+R3
      YNNN(2)=Y(2)+S3
      IF(YNNN(1).LT.0..AND.Y(2).GT.0.) GO TO 21
      CALL FCT(TNN,YNNN,DERY)
      R4=DERY(1)*DT
      S4=DERY(2)*DT
      DY1=(R1+2.*R2+2.*R3+R4)/6.
      DY2=(S1+2.*S2+2.*S3+S4)/6.
      Y(1)=Y(1)+DY1
      Y(2)=Y(2)+DY2
      T=TNN
      IF(ABS(T-BT)-1.) 80,80,81
   80 ACCE=DY1/DT/G
      WRITE(3,11) TNN,Y(1),Y(2),CD,DRAGF, ACCE
   11 FORMAT(1H0,4X,F8.2,4X,2(5X,E14.7),8X,F10.4,8X,E14.7,F10.3)
   81 IF(T.GT.BT.AND.Y(1).LE.0.) GO TO 21
      GO TO 4
   21 WRITE(3,22) T,Y(1),Y(2),DRAGF
   22 FORMAT(1H0,4HTIME,F7.2,7HSECONDS,5X,8HVELOCITY,E14.7,
     16HFT/SEC,5X,8HALTITUDE,E14.7,2HFT,5X,6HDRAGF=,E14.7)
      TW=TW+0.5
   50 CONTINUE
      VZERO=VZERO+200.
      40 CONTINUE
  101 STOP
      END

      SUBROUTINE FCT(T,Y,DERY)
      DIMENSION Y(2),DERY(2),YN(2),YNN(2),YNNN(2)
      COMMON AREA,CD,RHO1,ALPHA,   WFR,WF,BRATE,BT,G,A,B,C,ANUM,  RHO
     1      ,AMACH,TINF,A1,B1,C1,P1,ALPHA1,THAV,P
      IF(Y(2).LE.50000.) RHO=A+B*Y(2)+C*Y(2)**2
      IF(Y(2).GT.50000.) RHO=RHO1*EXP(ALPHA*Y(2))
      IF(Y(2).LE.50000.) P=A1+B1*Y(2)+C1*Y(2)**2
      IF(Y(2).GT.50000.) P=P1*EXP(ALPHA1*Y(2))
      IF(Y(2).GE.120000. .AND. Y(2).LE.164000.) TINF=450.+(Y(2)-120000.)
```

```
     1                                                    *18./4400.
      IF(Y(2).GT.164000. .AND. Y(2).LE.200000.) TINF=630.
      IF(Y(2).GT.200000. .AND. Y(2).LE.250000.) TINF=450.+(250000.-Y(2))
     1                                                    *18./5000.
      IF(Y(2).LT.120000. .OR. Y(2).GT.250000.) TINF=P/RHO/53.3
     SONIC = 49.02* SQRT(TINF)
      AMACH=Y(1)/SONIC
      IF(T.GT.BT) GO TO 80
      IF(AMACH.LE.0.9) CD=0.3
      IF(AMACH.GT.0.9.AND.AMACH.LE.1.2) CD=0.3+1.073*(AMACH-0.9)
      IF(AMACH.GT.1.2.AND.AMACH.LE.3.5) CD=0.321+.1309*(3.5-AMACH)
      IF(AMACH.GT.3.5.AND.AMACH.LE.5.5) CD=0.215+.053*(5.5-AMACH)
      IF(AMACH.GT.5.5) CD=.215
      CD1=CD
   80 IF(AMACH.LE.1.5) CD=.2+.3417*AMACH
      IF(AMACH.GT.1.5.AND.AMACH.LE.2.5) CD=.305+.1075*(2.5-AMACH)
      IF(AMACH.GT.2.5.AND.AMACH.LE.4.) CD=.25+.0366*(4.-AMACH)
      IF(AMACH.GT.4.) CD=.25
      IF(T.GT.BT) GO TO 60
      CD2=CD
      CD=CD2+(CD1-CD2)*BRATE
   60 ANUM=0.5*CD*AREA*RHO*Y(1)**2
   30 IF(T-BT) 61,61,62
   61 TT=T/BT
      IF(TT.LE.0.2) TSL=THAV*(0.953+1.03*TT)
      IF(TT.GT.0.2.AND.TT.LE.0.5) TSL=THAV*(1.265-0.53*TT)
      IF(TT.GT.0.5.AND.TT.LE.0.933) TSL=THAV*(1.0543-0.1086*TT)
      IF(TT.GT.0.933.AND.TT.LE.1.) TSL=THAV*(12.059-11.9*TT)
      TTOTAL=TSL+2.55*(2116.-P)/144.*BRATE
      TW=TTOTAL/WFR
      DENOM=WFR-BRATE*T
      DRAG=ANUM/DENOM
      DERY(1)=TW*G/(1.-BRATE*T/WFR)-DRAG-G
      DERY(2)=Y(1)
      IF(DERY(1).LE.0.0.AND.Y(2).LE.0.) GO TO 71
      RETURN
   71 DERY(1)=0.
      RETURN
   62 DENOM=WFR-WF
      DRAG=ANUM/DENOM
      DERY(1)=-DRAG-G
      DERY(2)=Y(1)
      IF(DERY(1).LE.0.0.AND.Y(2).LE.0.) GO TO 71
      RETURN
      END

DATA

      70.        4.45       315.       30.
```

REFERENCES

REFERENCES

1. Murray, J. J. and Kumar, S., "Vacuum-Air Missile Boost", American Rocket Society Journal 31, 1443-1445 (October 1961).

2. Rajan, J. R. N., "The Study of Motion of Projectiles in an Evacuated Tube and Propelled by Atmospheric Pressure", M. S. Thesis, Civil Engineering Department, Duke University, also ARO(D), Project Mountainwell, T. R. No. 1 (August 1962).

3. Kumar, S., Rajan, J. R. N., and Murray, J. J., "Vacuum-Air Missile Boost System", Journal of Spacecraft and Rockets, Vol. 1, No. 5, pp. 464-470 (September-October 1964).

4. Burr, J. W., Adair, W. R., and Madden, J. J., "Performance Analysis of the Murray-Kumar Missile-Boost System", TR AE 6110, Rensselaer Polytechnic Institute, Troy, New York (December 1961).

5. Lee, W. W., "Further Studies of the Vacuum-Air Missile Boost System", M. S. Thesis, Civil Engineering Department, Duke University, (September 1964).

6. Rajan, J. R. N., and Kumar, S., "Transient Subsonic Viscous Flow in the Vacuum-Air Propulsion System", ARO(D), Project Mountainwell, T. R. No. 5 (September 1966).

7. Chen, D., Kumar, S., Harman, C., and Buzzard, G., "Vacuum-Air Propulsion with a Supplemental Tube Inlet", ARO(D) Project Mountainwell, T. R. No. 8 (September 1968).

8. Foa, J. V., "Evaluation of the Increase of Missile Payload That Can Be Obtained from Atmospheric Boost at Take-off", ARO(D), Project Mountainwell, TR (September 1961).

9. Bryson, A. E., Jr., and Ross, S. E., "Optimum Rocket Trajectories with Aerodynamic Drag", Jet Propulsion, Vol. 28, pp. 465-469 (1958).

10. Leitmann, G., "Thrust Programming for High Altitude Rockets", Aeronautical Engineering Review, Vol. 16, No. 6, pp. 63-66 (1957).

11. Tsien, H. S., and Evans, R. C., "Optimum Thrust Programming for a Sounding Rocket", Jet Propulsion, Vol. 21, No. 5, pp. 99-107 (1951).

12. Goddard, R. H., "A Method of Reaching Extreme Altitude", Smithsonian Misc. Coll., Vol. 71, No. 2 (1919), and American Rocket Society (1946).

13. Scarborough, J. B., "Numerical Mathematical Analysis", 5th ed., The Johns Hopkins Press, 1962.

14. Shapiro, A. H., "The Dynamics and Thermodynamics of Compressible Fluid Flow", Vol. 1, The Ronald Press Co., 1953.

15. Ordway, F. I., III, and Wakeford, R. C., "International Missile and Spacecraft Guide", McGraw-Hill Book Company, Inc., 1960.

Unclassified

Security Classification

DOCUMENT CONTROL DATA - R & D

(Security classification of title, body of abstract and indexing annotation must be entered when the overall report is classified)

ORIGINATING ACTIVITY (Corporate author) U. S. Army Research Office-Durham	2a. REPORT SECURITY CLASSIFICATION Unclassified 2b. GROUP NA

3. REPORT TITLE

Performance and Optimization of Arcas and Other Single-Stage Rockets with Vacuum-Air Boost

4. DESCRIPTIVE NOTES (Type of report and inclusive dates)

Technical Report No. 9

5. AUTHOR(S) (First name, middle initial, last name)

Sudhir Kumar
Stanley Chin-nan Shieh

6. REPORT DATE	7a. TOTAL NO. OF PAGES	7b. NO. OF REFS
August 1969	75	15

8a. CONTRACT OR GRANT NO.	9a. ORIGINATOR'S REPORT NUMBER(S)
b. PROJECT NO. S-7-E	S-7.9-E
c.	9b. OTHER REPORT NO(S) (Any other numbers that may be assigned this report) NA
d.	

10. DISTRIBUTION STATEMENT

This document has been approved for public release and sale; its distribution is unlimited.

11. SUPPLEMENTARY NOTES	12. SPONSORING MILITARY ACTIVITY
	U. S. Army Research Office-Durham Box CM, Duke Station Durham, North Carolina 27706

13. ABSTRACT

Studies on optimization (altitude maximization) of a single-stage rocket performance with and without the use of the Vacuum-Air Missile Boost (VAMB) system are presented. Performance estimation and optimization of a hypothetical 1,000 lb rocket with and without the VAMB system have been done. Similar studies have also been performed for eighteen rockets of various countries without the VAMB system. It was found that the optimum thrust-to-weight ratio (T/W) for conventional rocket can be estimated roughly for preliminary design of rockets under simplifying assumptions. Detailed performance and optimization studies have been presented on the Arcas rocket. It was found that the optimum T/W for Arcas with and without VAMB system is approximately 2.4, which is almost half of the present design value (4.5). The gain in maximum altitude of the optimized Arcas launched with an initial velocity of 1,000 fps, over that of the present design Arcas without booster, was estimated to be nearly 93 per cent.

14. KEY WORDS

Boost	Pneumatic
Rocket	Propulsion
ARCAS	
Vacuum	

DD FORM 1 NOV 68 1473 REPLACES DD FORM 1473, 1 JAN 64, WHICH IS OBSOLETE FOR ARMY USE.

Unclassified